NONLINEAR MODEL PREDICTIVE CONTROL

OF MULTI-MACHINE POWER SYSTEM

BY

MOHAMMED MANSOOR BIN THABIT

A Thesis Presented to the

DEANSHIP OF GRADUATE STUDIES

KING FAHD UNIVERSITY OF PETROLEUM & MINERALS

DHAHRAN, SAUDI ARABIA

In Partial Fulfillment of the

Requirements for the Degree of

MASTER OF SCIENCE

In

ELECTRICAL ENGINEERING

December, 2013

KING FAHD UNIVERSITY OF PETROLEUM & MINERALS
DHAHRAN 31261, SAUDI ARABIA

DEANSHIP OF GRADUATE STUDIES

This thesis, written by **MOHAMMED BIN THABIT** under the direction of his thesis adviser and approved by his thesis committee, has been presented to and accepted by the Dean of Graduate Studies, in partial fulfillment of the requirements for the degree of **MASTER OF SCIENCE IN ELECTRICAL ENGINEERING**.

Thesis Committee

H. Duwaish
Dr. Hussain N. AL-Duwaish (Adviser)

Dr. Zakariya AL-Hamouz (Co-adviser)

Dr. Ahmad A. Masoud (Member)

Dr. Mohamed Mohandes (Member)

Dr. Salim Ibrir (Member)

Dr. Ali Ahmad AL-Shaikhi
Department Chairman

Dr. Salam A. Zummo
Dean of Graduate Studies

4/5/14
Date

عمادة الدراسات العليا
DEANSHIP OF GRADUATE STUDIES

To the loving memory of my mother

To my beloved father

To my family

ACKNOWLEDGMENTS

All praise and gratefulness are due to Allah, the Most Merciful, the Most Beneficent. He has guided me to complete this work. My humblest gratitude also to Prophet Muhammad, peace be upon him, and to his family and his companions.

I would like to express my extreme gratitude to King Fahd University of Petroleum and Minerals and the Hadhramout Establishment for Human Development (HEHD) for awarding me the scholarship and for providing me various facilities to pursue my master's program.

My special appreciation and thanks to my advisor Dr. Hussain N. AL-Duwaish and co-advisor, Dr. Zakariya M. Al-Hamouz. Thank you for your guidance to make this work possible, your helpful comments and insights, your patience, and your encouragement. I would like to thank the rest of my thesis committee, Dr. Ahmad A. Masoud, Dr. Mohamed Mohandes, and Dr. Salim Ibrir for their feedback, direction, and assistance through this work.

Warm thanks to my family, especially to the soul of my beloved mother to whom I can not express my gratitude in words to her. May Allah the most Merciful forgive her sins and grant her a place in Paradise. She was the first teacher in my life and she was a candle lighting my life. Deep heart-felt thanks to

my father for his constant support, his endless encouragement, and his valuable advice at every stage in my life. Sincere thanks go to my brother Bader, my sisters, my wife, and my son Hatim for continued support and for providing a loving environment for me.

All thanks to the many people who have been a part of my education, namely my teachers, friends, and colleagues for their unconditional support.

TABLE OF CONTENTS

LIST OF TABLES

LIST OF FIGURES

LIST OF ABBREVIATIONS

NMPC	:	Nonlinear Model Predictive Control
MMPS	:	Multi-Machine Power System
SMIB	:	Single Machine Infinite Bus
PID	:	Proportional−Integral−Derivative
MPC	:	Model Predictive Control
FACTS	:	Flexible AC Transmission System
EP	:	Evolutionary Programming
GA	:	Genetic Algorithm
PSO	:	Particle Swarm Optimization
TCSC	:	Thyristor Controlled Series Capacitor
STATCOM	:	Static Compensator
GPC	:	Generalized Predictive Control
PSS	:	Power System Stabilizer
AVR	:	Automatic Voltage Regulator
EEAC	:	Extended Equal Area Criterion

LMPC	:	Linear Model Predictive Control
DMC	:	Dynamic Matrix Control
IMC	:	Internal Model Control
LRPC	:	Long Range Predictive Control
KKT	:	Karush-Kuhn-Tucker
WSCC	:	Western System Coordinated Council

THESIS ABSTRACT

NAME: Mohammed Bin Thabit

TITLE OF STUDY: Nonlinear Model Predictive Control of Multi-Machine Power System

MAJOR FIELD: Electrical Engineering

DATE OF DEGREE: December, 2013

This thesis presents the application of Nonlinear Model Predictive Control (NMPC) on Multi-Machine Power System (MMPS) to improve the transient stability which is considered as a major concern in power systems operation. Nonlinear Model Predictive Control is applied to solve the problem of degradation of transient stability of MMPS in the presence of large disturbances and physical constraints that may violate the stability. The strength of NMPC to handle the nolinearity and the constraints of the system made it more suitable for implementation on MMPS.

The transient stability is studied first on the Single Machine Infinite Bus (SMIB) and then, extended to MMPS under the following large disturbances: three phase fault, load changing, and mechanical power changing. A comparison between this study and what was achieved in previous work on the same topic showed that the proposed NMPC with Active-set algorithm as an optimizer is more capable of bringing the system to equilibrium than the previous work. The robustness of the proposed controller has been examined against the variations of system parameters.

Keywords: *Nonlinear Control, Model Predictive Control, Active-set algorithm, Transient Stability, Single Machine Infinite Bus, Multi-machine Power System, 3-Machines 9-bus WSCC System.*

ملخص الرسالة

الاسم الكامل: محمد منصور بن ثابت

عنوان الرسالة: نظام التحكم التنبئي اللاخطي لأنظمة الطاقة متعددة الآلات

التخصص: الهندسة الكهربائية

تاريخ الدرجة العلمية: ديسمبر ٢٠١٣ م

هذه الأطروحة تقدم تطبيق نظام التحكم التنبئي اللاخطي (NMPC) على أنظمة الطاقة متعددة الآلات (MMPS) و ذلك لتحسين من الإستقرارية العابرة و التي تعتبر إحدى أكثر الإهتمامات في تشغيل أنظمة الطاقة. نظام التحكم التنبئي اللاخطي طبق من أجل إجاد حل لمشاكل الإنحدار في الإستقرارية العابرة لـ (MMPS) في ظل وجود الإضطرابات العالية و كذلك في ظل وجود القيود الفيزيائية و التي قد تحدث عدم الإستقرار. إمكانية (NMPC) على التعامل مع عدم الخطية و القيود جعله أكثر ملائمة لتطبيقه على (MMPS).

تم دراسة الإستقرارية العابرة أولا على الآلة الأحادية للخط اللانهائي (SMIB) ، و من ثم طبق على (MMPS) تحت الإضطرابات العالية التالية: خطأ النظام الثلاثي و تغيير الحمل و تغيير الطاقة الميكانيكية. مقارنة بين هذا البحث و ماتم التوصل اليه من البحوث السابقة في هذا المجال اظهرت ان الـ(NMPC) مع (Active-set algorithm) كمحسن قادر على جعل النظام يعود الى نقطة التوازن مقارنة بالبحوث السابقة. تم اختبار قدرة التحكم المقترح مع التغييرات في معطيات النظام.

CHAPTER 1

INTRODUCTION

1.1 Motivation

Conventional Proportional-Integral-Derivative (PID) controller has dominated the process control for the past four decades, where the PID controller directly compares the output data value with a reference data value and uses the compared error for the input in order to minimize it and keep the output data at the setpoint. Although the PID controller is simple, fast, and easy to tune and implement in hardware and software, it has some limitations, especially when the system is more complex which means more multi-variables. The other limitation is when the system variables have constraints in their values.

Model Predictive Control (MPC) deals with the systems which have multi-variable and constraints on their variables. MPC becomes a powerful control, not just in process control, but also in other areas including power systems. In the last two decades, the applications of MPC in power systems have attracted many

researchers. One of these applications is to improve the transient stability of power systems. Transient stability determines the power system's ability to tackle severe disturbances that may occur such as the trip of a transmission line without the loss of synchronism and with its return to a state of equilibrium following these disturbances.

MPC applied to Single Machine Infinite Bus is provided as a simple example, in order to test the transient stability of the power system. Over recent years, there has been more focus on the linear and nonlinear Model Predictive Control to SMIB which has shown good results in handling disturbances and satisfying the constraints of the power system.

In the literature, only a little work has been written about the application of the Nonlinear Model Predictive Control on Multi-Machine Power Systems. Most of these studies concern the use of only a second order system for each machine, with the help of Flexible AC Transmission System (FACTS) devices to improve the transient stability.

In this study we will firstly apply the NMPC to SMIB and then we will extend it to MMPS in order to enhance the transient stability. Each one of MMPS will be represented by a third order model, in order to make the control possible by using the excitation voltage as an input. At the same time, the study will take into consideration the imposed constraints and the nonlinearity of the model.

1.2 Problem Formulations and Objectives

This thesis will design an NMPC controller for Single Machine Infinite Bus and then it will extend to a Multi-Machine Power System in order to enhance the transient stability suffering from the following large disturbances:

1. Three phase fault applied to transmission lines.

2. System load changing.

3. Mechanical power changing.

The objective of using NMPC controller due to its ability to handle the nonlinearity and the constraints that may be imposed due to physical limits. Thus, this thesis will have the following objectives:

1. Improve the stability of both SMIB and MMPS.

2. Satisfy the imposed constraints of both SMIB and MMPS.

3. Study the MMPS system under some cases of disturbance.

1.3 Thesis Organization

This thesis is divided into six chapters. In the first chapter, the motivation of this work and the problem definition are addressed.

The second chapter explores the literature review of both Single Machine Infinite Bus and Multi-machine Power System.

In the third chapter, an essential historical overview of the Model Predictive Control and introduction of its theory and algorithm are addressed. Active set Algorithm, advantages and disadvantages of MPC, and MPC tuning parameters are discussed.

In chapter 4, NMPC applied to highly nonlinear SMIB system for three cases: without constraints, with constraints, and robustness of NMPC controller. The comparison between the results of NMPC framework achieved in this thesis and the results given in [1] are discussed.

In Chapter 5, NMPC is applied to MMPS for different cases of large disturbances including: three phase fault, system load changing, and mechanical power changing. In the case of three phase fault, a comparison between the results of NMPC framework achieved in this thesis and state feedback controller given in [2] are discussed.

In Chapter 6, the summary of results and the future work that can be done to the proposed controller are discussed.

CHAPTER 2

LITERATURE REVIEW

2.1 Single Machine Infinite Bus

In the literature, several methods are applied in order to control the SMIB system. Some of these methods are classical control [3], optimal control [4], adaptive control [5], and variable structure control [6].

MPC applied to Single Machine Infinite Bus is provided as a simple example, in order to test the transient stability of the power system. Over recent years, there has been more focus on the linear and nonlinear Model Predictive Control to SMIB which has shown good results in handling disturbances and satisfying the constraints of the power system.

Linear MPC (LMPC) considered for stabilization of SMIB [7, 8, 9, 10, 11]. Most of these references used MPC control with the help of Flexible AC Transmission Systems (FACTS).

In the last two decades, many applications of NMPC have been addressed to the power systems. Some of these applications are on Fossil Fuel Power Units [12, 13, 14], Wind Turbines [15, 16, 17, 18], Power Boilers [19, 20], Rectifiers and Converters [21, 22, 23].

In the literature NMPC has been applied to SMIB. Yousuf and his advisors, Al-Hamouz and Al-Duwaish [24, 25] presented the combinations of heuristic optimization algorithms as Evolutionary Programming (EP), Genetic Algorithm (GA) and Particle Swarm Optimization (PSO) as optimizers of MPC offer the advantage of finding the optimal control without need for linearization. Nonlinear Predictive Control with based FACTS devices of SMIB are applied to improve SMIB stability. Wagh et al [26] improved the transient stability by using NMPC based on Thyristor Controlled Series Capacitor (TCSC) controller by linearizing the model at each instant of time. In a different work, Wagh et al [27] presented the nonlinear control of based TCSC controller with both Control Lyapunov Function and receding horizon strategy. [28] proposed a control for Static Compensator (STATCOM) based on nonlinear Generalized Predictive Control (GPC), improving power system stability and voltage regulation.

In this work, the proposed NMPC control is applied to SMIB without need to linearization and with no use of FACTS devices.

2.2 Multi-machine Power System

With the large power network and with the presence of oscillations that may affect the stability of power system, there was a need to damp these oscillations. For MMPS a lot of work has been done in order to reduce the effects of these oscillations. One of the methods employed to reduce the oscillations is the use of supplementary controllers like Power System Stabilizer (PSS) and Automatic Voltage Regulator (AVR). Several techniques are used to design PSS like Conventional [29, 30, 31, 32], Optimal [33, 34], Adaptive [35, 36, 37], H-based [38, 39], Variable Structure [40, 41], and Intelligent and Heuristic techniques [42, 43, 44].

In the last decade, more concern has been paid to address the Linear and Nonlinear Model Predictive Control to MMPS, which showed a good improvement to handle the disturbances and satisfy the constraints of power system.

Linear MPC considered for stabilization of MMPS. Li et al [45] used Generalized Predictive Control for emergency control of transient stability based on the Extended Equal Area Criterion (EEAC). Soos and Malik [46] identified the time varying model of MMPS by robust control followed by H_∞ control design and studied different cases for the use of MPC with and without PSS. Wu and Malik in [47] proposed a multivariable adaptive power system stabilizer based on a recursive subspace identification method and generalized predictive control strategy. Ye and Liu in [48] proposed an adaptive damping controller design method by integrating online recursive closed-loop subspace model identification

with model predictive control theory. It is different from [47] in two ways. First, an online recursive closed-loop subspace identification method. Second, it focuses on damping inter-area oscillation modes. MPC control with FACTS devices is used to improve MMPS stability [49, 50]. A Distributed MPC demonstrated the transient stability in [51] and voltage control [52, 53]. Qudaih et al [54] presented the MPC technique in order to robustly tune the power system stabilizer and automatic voltage regulator. Generalized Predictive Control with the use of hybrid shuffled frog leaping as optimizer is used in [55].

Nonlinear MPC addressed to MMPS, Rajkumar and Mohler [56] presented a framework for the development of discrete-time, nonlinear Generalized Predictive Control using coordination control of TCSC for the stabilization and rapid damping of MMPS which are subjected to large disturbances. In this strategy for large faults nonlinear predictive controller with a small prediction horizon is designed to return the power system state to a small region approaching the post-fault equilibrium. In this region, the linear controller can be designed to provide local asymptotic stabilization. Zima and Andersson [57] presented a formulation of MPC for controlling reactive power and voltages of MMPS based on trajectory sensitivities. Emergency voltage control of power system based on search and NMPC approaches are presented in [58]. Ford et al [59] presented the NMPC control with short horizon by choosing an appropriate terminal cost function to achieve the first swing transient stability of MMPS.

Most of the previous studies concern the use of only a second order system for each machine, with the help of FACTS devices to improve the transient stability. In this study, each one of MMPS will be represented by a third order model, in order to make the control possible by using the field winding signal as an input. At the same time, the study will take into consideration the imposed constraints and the nonlinearity of the model.

CHAPTER 3

MODEL PREDICTIVE CONTROL BACKGROUND

In this chapter, an essential literature review of the Model Predictive Control, introduction of its theory and algorithm, and advantages and disadvantages of MPC are discussed.

3.1 MPC Historical Overview

The beginning of LMPC was in the late 1970s, where in 1978 Richalet et al. described the applications of "Model Predictive Heuristic Control" [60]. In 1979 engineers from Shell demonstrated "Dynamic Matrix Control" (DMC) and reported its applications to a fluid catalytic cracker [61]. The Generalized Predictive Control is given by Clarke et al. in 1987 which was intended to provide a new adaptive control alternative [62] and then the Internal Model Control (IMC) was outlined by Garcia and Morari [63]. The main differences for all previous MPC

algorithms are the types of models used to represent the plant dynamic and the cost function to be minimized [64]. In 1988, Keyser et al., presented a comparative study of self-adaptive Long Range Predictive Control (LRPC) methods keeping focus on robustness with respect to unmodeled dynamics, parameter variations, process noise and varying dead-time [65].

For good reviews about linear MPC, numerous excellent technical reviews of MPC that provide more details about MPC formulation and its future directions from an academic perspective [66, 67, 68], and from an industrial perspective [69, 70, 71] are available.

Nonlinear Model Predictive Control has attracted more attention over the recent years. The earliest paper which analyzed an NMPC algorithm like we use today was given by Chen and Shaw [72] in 1982.

NMPC's computational problem has been an active research issue for the last two decades and several methods have been developed and reported. One of these methods is the model order reduction approach. This approach is assigned to deal with large systems to reduce the computation of differential equations. Orthogonal Collocation method is the famous method in order reduction approach [73] and [74]. The model order is reduced by converting a differential equation in the time domain into an approximating set of algebraic equations. Rather than using model order reduction approach, some researchers chose to increase the speed of popular local optimization method by taking advantage of the specific structure

of the MPC formulation. The interior-point approach considered to be a good example for this. This method was successful in easing the computation in NMPC and has found favor with many academic researchers lately [75]. For the non-convex problem, the computation is focused on global optimization, especially the genetic algorithms [76, 77]. Another research direction is to simplify the optimization problem in order to decrease the computation time of each calculation. One method proposed by Zheng [78] is to optimize only the first move of the prediction horizon instead of performing the optimization all along the control horizon. However, this approach does not give the desired results as it is closely related to a finite horizon optimization with one step ahead prediction.

For further details about NMPC, many theoretical and practical issues have been reported in [79, 80, 81, 82, 83].

3.2 MPC Theory and Algorithm

From references [83, 84] we can find the basic principle of Model Predictive Control. Generally, MPC can be defined as solving on-line a finite horizon open-loop optimal control problem subject to system dynamics and constraints involving states and controls.

For nonlinear control system of the form:

$$x(k+1) = f(x(k), u(k)), \quad x(0) = x_0 \tag{3.1}$$

subject to inputs and states:

$$u(k) \in U \tag{3.2}$$

$$x(k) \in X \tag{3.3}$$

where U and X are the input and state vectors respectively.

The cost function to be minimized:

$$J_N = \sum_{k=0}^{N-1} F(x(k), u(k)) \tag{3.4}$$

where

$$F(x(k), u(k)) = (x(k) - x_s(k))^T Q(x(k) - x_s(k)) + u(k)^T R u(k) \tag{3.5}$$

x_s denote given setpoint.

Q and R denote positive definite, symmetric weighting matrices.

The model is subjected to the following constraints imposed on inputs and states respectively:

$$-u_{min} \leq u_k \leq u_{max} \tag{3.6}$$

$$-x_{min} \leq x_k \leq x_{max} \tag{3.7}$$

NMPC approach can be summarized as follows:

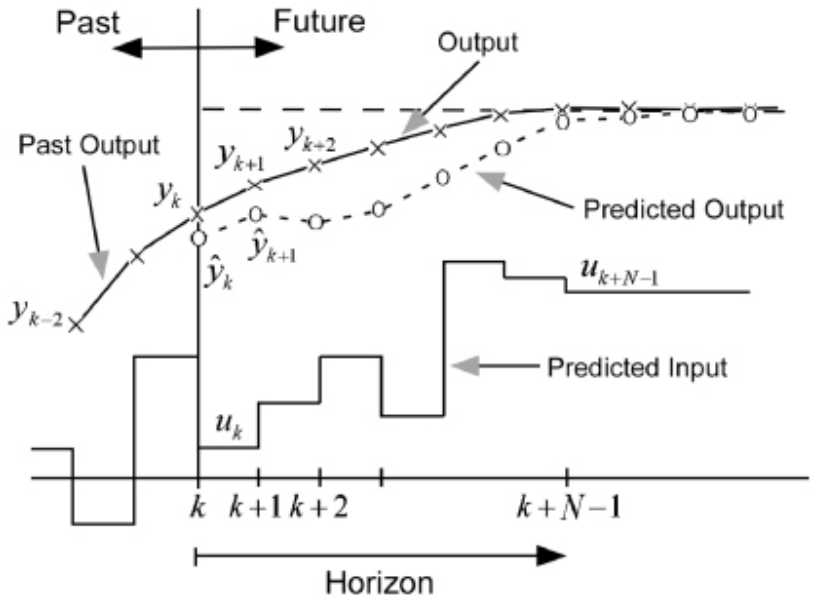

Figure 3.1: Principle of MPC.

1. Estimate the states of the system for the prediction horizon (N) at each instant k.

2. An optimal input minimizing the desired cost function over the prediction horizon (N) using the system model for prediction is calculated.

3. The first part of the optimal input is implemented until the next sampling instant.

4. Continue with (1).

Figure 3.1 shows the principle of MPC for one horizon which is moving for the next calculation and the term 'Moving Horizon' derives from this.

The solution of NMPC consists of two essential procedures:

1. Solving the optimization problem to find the optimum control.

2. Integrating the model equations which could be differential with algebraic or empirical model.

3.3 Active set Algorithm

The active set algorithm is selected to solve the optimization problem in this thesis, because the active-set algorithm is suited to optimize inequality constraints of Quadratic Programing [85] and the imposed constraints of both SMIB and MMPS are inequality constraints. The optimization problem is solved using the function "fmincon" from MATLAB® Optimization Toolbox.

In literature, the active set algorithm addressed to solve the optimization problem of NMPC [86, 87, 88].

A brief overview of active set algorithm is given from the references [85, 68]. The objective function is expressed

$$min\ q(x) = \frac{1}{2}x^T Gx + x^T d \tag{3.8}$$

subject to equality and inequality constraints

$$Ax = b \tag{3.9}$$

$$Ax \leq b \tag{3.10}$$

where

x: The decision variable.

G, d, A and b are compatible matrices and vectors in the quadratic programming problem. G is assumed to be a symmetric and positive definite.

The Lagrange expression of objective function subject to only the equality constraints is given as:

$$q(x) = \frac{1}{2}x^T Gx + x^T d + \lambda^T (Ax - b) \tag{3.11}$$

The procedure of minimization is to take the first partial derivatives with respect to the vectors x and λ. This gives us the results

$$\frac{\partial q}{\partial x} = Gx + d + A^T \lambda \tag{3.12}$$

$$\frac{\partial q}{\partial \lambda} = Ax - b \tag{3.13}$$

The optimal values of λ and x are found by equating the equations 3.12 and 3.13 to zero:

$$\lambda = -\left(AG^{-1}A^T\right)^{-1}\left(b + AG^{-1}d\right) \tag{3.14}$$

$$x = -G^{-1}\left(A^T\lambda + d\right) \tag{3.15}$$

The active and inactive constraints are defined from Karush-Kuhn-Tucker (KKT) conditions in terms of the Lagrange multipliers (λ's). The necessary con-

ditions of KKT are:

$$Gx + d + \sum_{i \in S_{act}} \lambda_i a_i = 0 \tag{3.16}$$

$$a_i^T x - b_i = 0, \quad i \in S_{act} \tag{3.17}$$

$$a_i^T x - b_i < 0, \quad i \notin S_{act} \tag{3.18}$$

$$\lambda_i \geq 0, \quad i \in S_{act} \tag{3.19}$$

The idea of active set methods is to define a set of constraints at each step of an algorithm , termed the working set, that is to be considered as the active set. The algorithm then proceeds to move on the surface defined by the working set of constraints to an improved point. At each step of the active set method, an equality constraint problem is solved. If all the Lagrange multipliers $\lambda_i \geq 0$, then the point is a local solution to the original problem. If, on the other hand, there exists a $\lambda_i \leq 0$, then the objective function value can be decreased by deleting the constraint i. During the minimization, it is necessary to monitor the values of the other constraints to be sure that they are not violated, since all points defined by the algorithm must be feasible.

Euler method is used to solve the differential equations of the models of SMIB (equation 4.10) and MMPS (equations 5.1, 5.2, and 5.3). Euler method has the general form

$$x_{i+1} = x_i + hf(x_i, t_i) \tag{3.20}$$

where

h is the step size.

3.4 MPC Tuning Parameters

The MPC controller can be tuned by the following parameters [89]:

- Prediction horizon (N).
- Sampling time Δt.
- Weighting matrix for predicted errors (Q).
- Weighting matrix for control moves (R).

3.5 MPC advantages and disadvantages

Model Predictive control used extensively in process control due to the following advantages [84, 90]:

- Capable of handling processes with large number of manipulated and controlled variables.
- Allows the constraints to be imposed on both manipulated and controlled variables.
- The process model captures the dynamic interactions between input and output.
- Allows use of linear and nonlinear models.

- Accurate model predictions can provide early warnings of potential problems.

Despite the advantage of MPC, there are also some disadvantages [64, 91, 92]:

- Optimization must happen in real-time.
- MPC controllers require a large number of tuning parameters.
- MPC is an open methodology. For different predictive controllers, each can have different properties and might not work with another process.

CHAPTER 4

APPLICATION OF NONLINEAR MODEL PREDICTIVE CONTROL ON SINGLE MACHINE INFINITE BUS

In this chapter, NMPC controller is applied to the Single Machine Infinite Bus system. Different scenarios of operation are studied.

4.1 Nonlinear Model of SMIB

The nonlinear model of SMIB is given in [1] and the diagram representing the physical components of SMIB is shown in Figure 4.1.

The mathematical model describing the dynamics of the system requires the following assumptions:

- The voltage behind the transient reactance is considered to be a constant.
- A slow first-order system is used to describe the governor/turbine dynamics.
- The mechanical motion of the machine is represented by the swing equations.

The nonlinear dynamic of SMIB is described by the following equations [1]:

$$\dot{\delta} = \omega \tag{4.1}$$

$$\dot{\omega} = \frac{\omega_B}{2H}\left[P_m - P_{ac} - KP_{dc}\right] - D.\omega \tag{4.2}$$

$$\dot{I}_d = \frac{1}{L}\left(cos(\beta) - R_c I_d\right) \tag{4.3}$$

$$\dot{P_m} = -\alpha P_m + v \tag{4.4}$$

$$P_{dc} = \left(cos(\beta) - R_c I_d\right) I_d \tag{4.5}$$

$$P_{ac} = \left(\frac{E_1 E_2}{X}\right) sin(\delta) \tag{4.6}$$

$$X = X_d + X_t + X_l \tag{4.7}$$

where:

δ: Rotor angle of the machine in rad.

ω: Rotor angular velocity in rad/sec.

P_m: Mechanical Power in $p.u$.

P_{ac}: AC power in $p.u$.

P_{dc}: DC power stored in the converter in $p.u.$

H: Inertia constant in $sec.$

D: Damping factor in $sec^{-}1.$

I_d: Direct Current in $p.u.$

R_c: Commutating resistance $p.u.$

β: SCR firing angle.

α: Time constant of governor/turbine or mechanical power actuator.

v: The input to governor/turbine.

$K = 1$

$\omega_B = 377\ rad/s.$

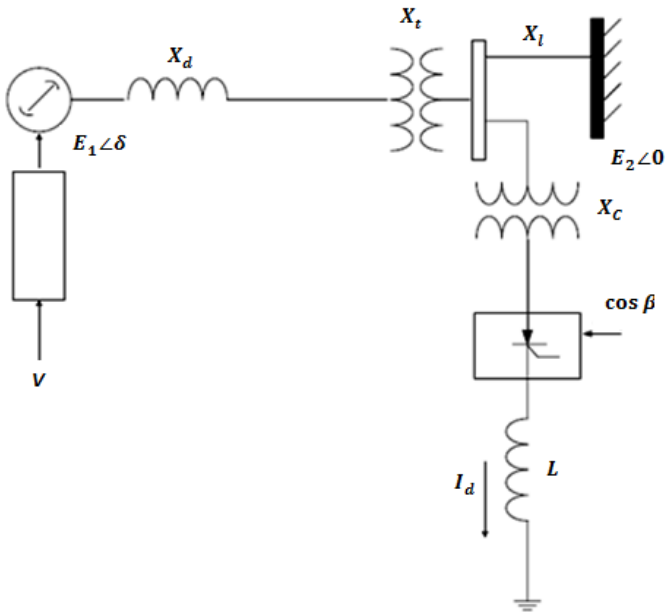

Figure 4.1: Diagram of Single Machine Infinite Bus (SMIB).

The states of the system are defined as follows:

$$\begin{bmatrix} x_1 \\ x_2 \\ x_3 \\ x_4 \end{bmatrix} = \begin{bmatrix} \delta \\ I_d \\ \omega \\ P_m \end{bmatrix} \tag{4.8}$$

Where the control inputs are defined as:

$$\begin{bmatrix} u_1 \\ u_2 \end{bmatrix} = \begin{bmatrix} cos(\beta) \\ v \end{bmatrix} \tag{4.9}$$

where

β: SCR firing angle.

v: the input to governor/turbine.

The nonlinear model of perturbed SMIB defined in equations (4.1, 4.2, 4.3 and 4.4) can be performed in state space form as follows:

$$\begin{bmatrix} \dot{x_1} \\ \dot{x_2} \\ \dot{x_3} \\ \dot{x_4} \end{bmatrix} = \begin{bmatrix} x_3 \\ -k_1 x_2 \\ -k_2 sin(x_1) + k_3 {x_2}^2 - D x_3 + k_5 x_4 \\ -\alpha x_4 \end{bmatrix} + \begin{bmatrix} 0 & 0 \\ k_4 & 0 \\ -k_5 x_2 & 0 \\ 0 & 1 \end{bmatrix} \begin{bmatrix} u_1 \\ u_2 \end{bmatrix} \tag{4.10}$$

where:

$k_1 = \frac{R_c}{L}$, $k_2 = \frac{\omega_B E_1 E_2}{2HX}$, $k_3 = \frac{\omega_b R_c}{2HX}$, $k_4 = \frac{1}{L}, k_5 = \frac{\omega_B}{2H}$

As stated in [1] the DC Converter is rated at 80 MW. The system is 230 kV and the machine rating is 800 MVA. On this rating base, the system parameters are : $\omega_B = 377$ rad/s, $\omega_b = 75.399$ rad/s, $X = 0.2$ p.u, $R_c = 0.3$ p.u, $L = 0.015$ p.u, $H = 7.0$ s, $D = 0.5\ s^{-1}$, and $\alpha = -0.1\ s^{-1}$.

Thus, the constants used in equation (4.10) are given as:

$$k_1 = 20,\ k_2 = 177.72857,\ k_3 = 8.078571,$$

$k_4 = 66.667$, and $k_5 = 26.928561$.

4.2 Design of NMPC Control for SMIB

The main control goal is to bring the system from a perturbed state to a equilibrium point and keep it there without violating the constraints imposed on both states and control input. The specific goals of control are:

- The machine must be operated at the rated frequency, i.e. change in machine speed, x_3 must be zero at equilibrium.
- The DC current through the converter, x_2 must be zero at equilibrium.

The SMIB system is already in perturbed state with the following initial condition [1]:

$$x_1 = 0.0522,\ x_2 = 0.1,\ x_3 = 0.1\ \&\ x_4 = 6.6sin(x_1(0)) = 0.3444 \tag{4.11}$$

The constraints are assigned to the states and control inputs as follows [1]:

$$0 \leq x_2 \leq 0.1 \tag{4.12}$$

$$x_4 \geq 0 \tag{4.13}$$

$$-0.95 \leq u_1 \leq 0.985 \tag{4.14}$$

$$-3.5 \leq u_2 \leq 3.5 \tag{4.15}$$

The objective function to achieve the desired control goals is stated as:

$$J = \sum_{k=0}^{N-1} \omega^2(k) + \ I_{dc}^2(k) \tag{4.16}$$

where:

N: The prediction horizon.

ω: The frequency deviation.

I_{dc}: The DC current converter.

4.3 Performance of NMPC on SMIB

In this section, various cases of NMPC control of SMIB are discussed to study the performance of the proposed controller. All simulations in this thesis are run on MATLAB® on an Intel Core i5 CPU @2.53GHz with 6GB of RAM. Different values of prediction horizon (N) and sampling time (Δt) have been tried and compromised values were found to be $N = 0.1$ s and $\Delta t = 0.002$ s for all cases of simulation.

As stated in section (3.3) the active set algorithm is selected to solve the optimization problem using function "fmincon" from MATLAB® Optimization Toolbox.

4.3.1 Case 1: SMIB without constraints

In this case, the system of SMIB is studied with no constraints imposed on either the states (x_2, x_4) or the controls (u_1, u_2). This leads the control effort to take any value to bring the system from perturbed initial state given in Equation 4.11 to equilibrium.

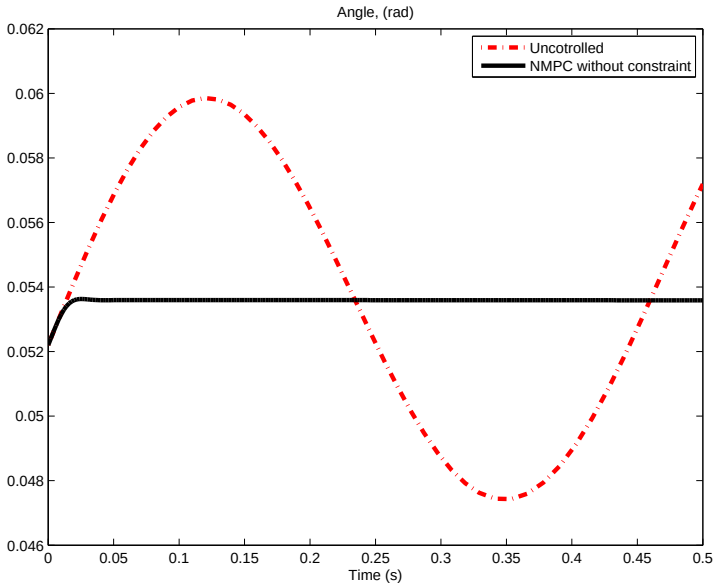

Figure 4.2: Rotor Angle Case 1

Figures 4.2, 4.3, 4.4, 4.5 show the system states without control and with NMPC controller. From figures 4.3 and 4.4, the converter current, x_2 (I_{dc}) and the frequency deviation, x_3 (ω) reached the equilibrium as stated in the control goals at 0.02 s and 0.05 s respectively. The rotor angle, x_1 (δ) in figure 4.2 takes a value (about 0.05359 rad) to reach the steady state at 0.05 s. Mechanical power, x_4 (P_m) takes a minimum value 0.106 p.u and goes to overshoot slightly with 0.37 p.u before it converges to equilibrium at value of 0.353 p.u.

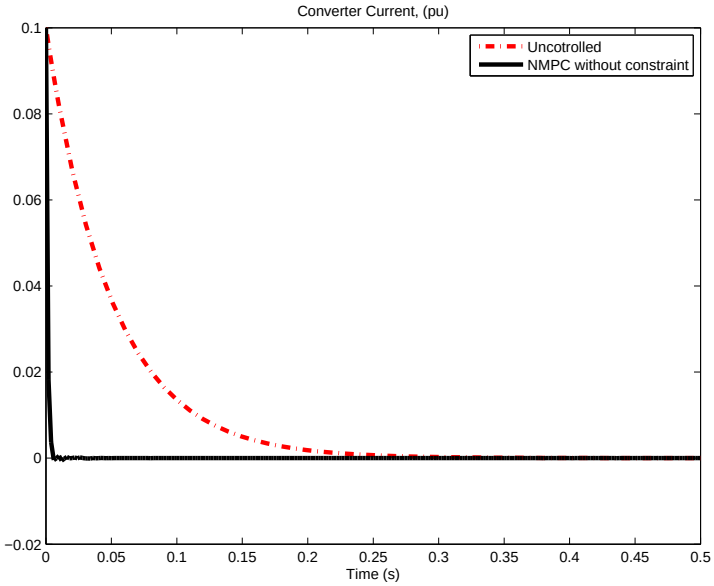

Figure 4.3: Converter Current Case 1.

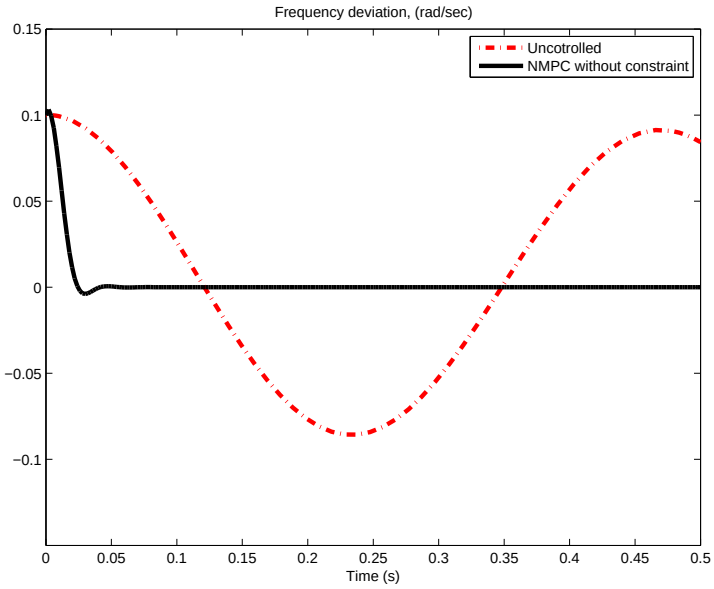

Figure 4.4: Frequency Deviation Case 1.

The control inputs u_1 $(cos(\beta))$ and u_2 (V) are shown in Figures 4.6 and **??**. It is shown that the control effort of u_1 starts with a minimum value of -0.583 and then goes to increase rapidly and then settles to zero at 0.05 s. The control effort of u_2 begins with a minimum value of -32.28 and then increases to a maximum

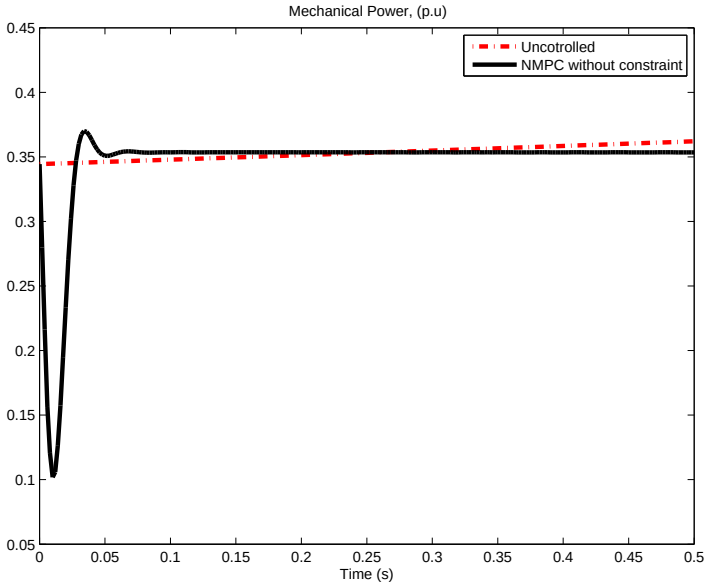

Figure 4.5: Mechanical Power Case 1.

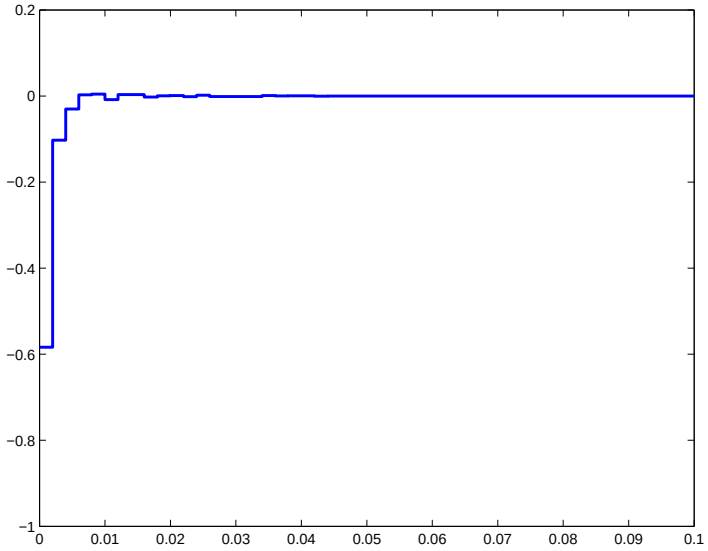

Figure 4.6: $u1$, $cos(\beta)$ Case 1.

value 19.29 before it converges to zero.

4.3.2 Case 2: SMIB with constraints

In this case, the constraints are imposed as stated in constraint equations 4.12, 4.13, 4.14, and 4.15 and the system should be stay within these limits. The

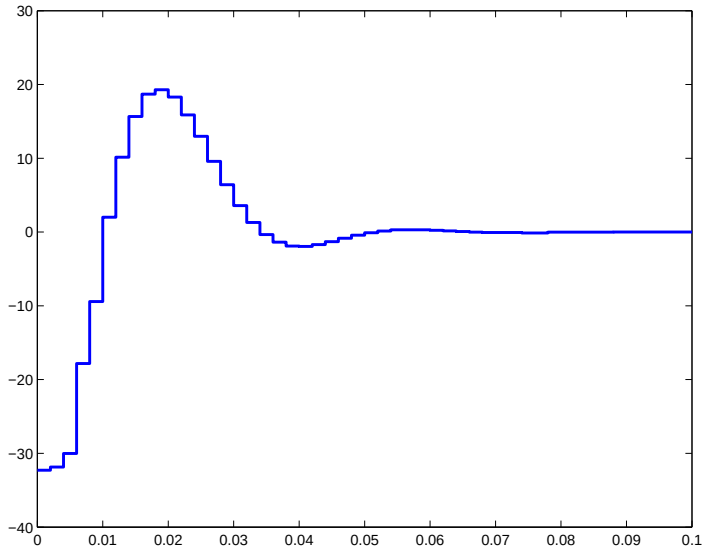

Figure 4.7: $u2$, v comparison between VSC [1] and NMPC.

objective of control is to bring the frequency, x_3 and DC current of converter, x_2 from a perturbed initial state to a desired equilibrium (zero) with imposed constraints.

It is shown from figures 4.8, 4.9, 4.10, and 4.11 that the system takes more time to converge to the equilibrium compared to when the system has no constraints. This is because of the limitations on the states and control efforts. With constrained system, the frequency deviation in figure 4.10 goes to zero in 0.08 s compared to 0.05 s without constraints. The current converter in figure 4.9 settles to equilibrium in 0.015 s. It is seen that the NMPC controller has succeeded to achieve the control goals with imposed constraints.

The rotor angle in figure 4.8 goes to a steady state value of 0.05537 rad in 0.074 s with the constrained system, whereas without constraints the system goes to a steady state value of 0.05359 rad in 0.05 s. The mechanical power in figure

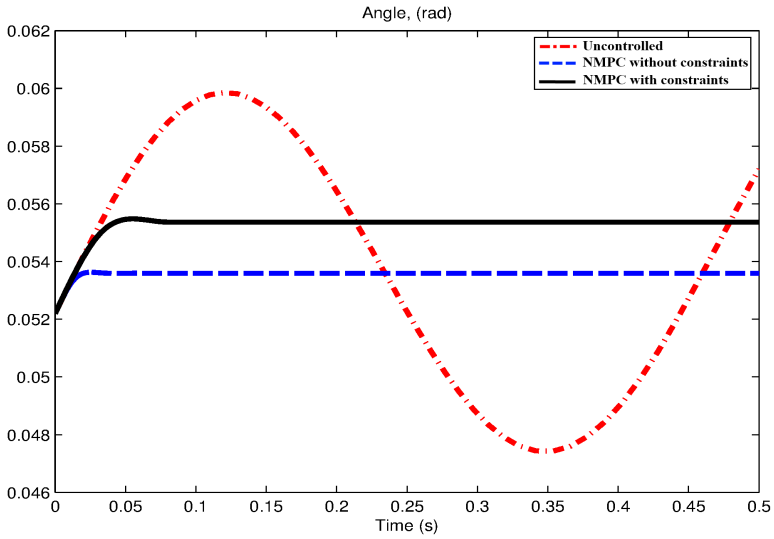

Figure 4.8: Rotor Angle Case 2

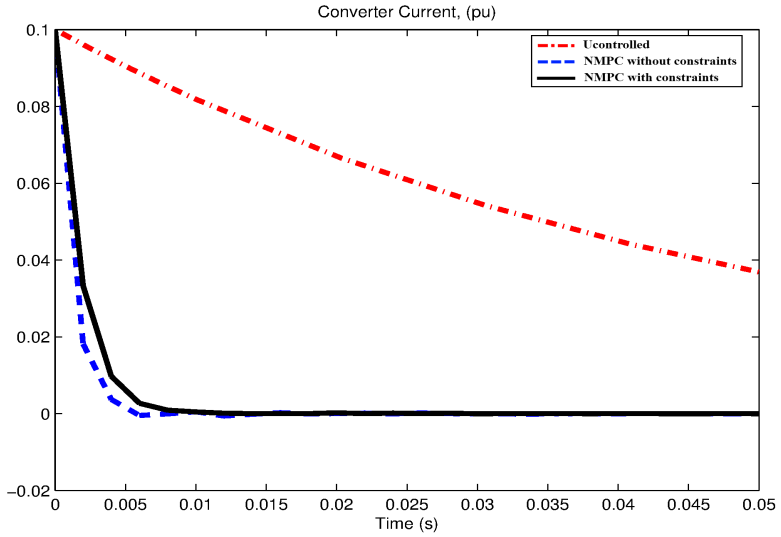

Figure 4.9: Converter Current Case 2.

4.11 settles with a value of 0.3653 p.u with constrained system and to 0.353 p.u without constraints. It can be noticed from the rotor angle and mechanical power responses that the machine produced more mechanical power when the constraints are imposed compared with no constraints in order to adapt the restrictions.

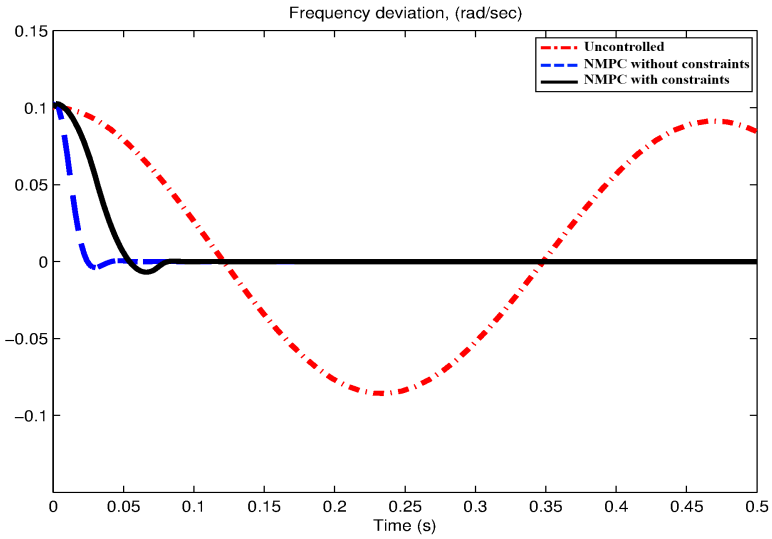

Figure 4.10: Frequency Deviation Case 2.

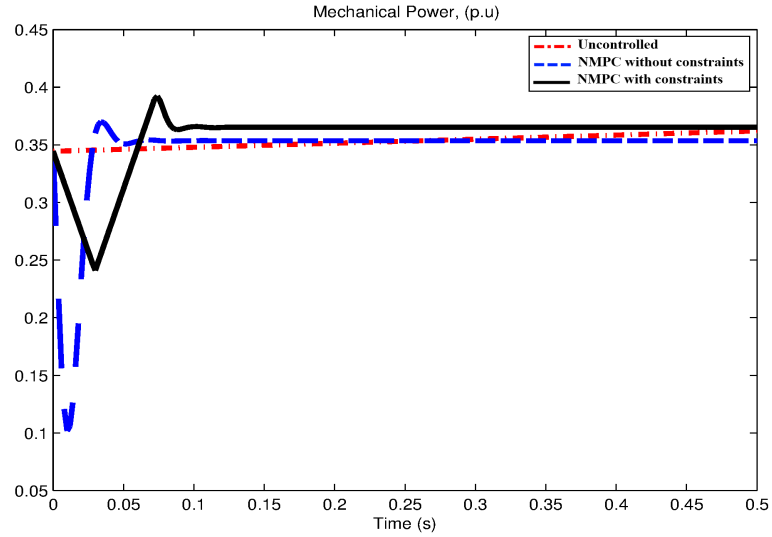

Figure 4.11: Mechanical Power Case 2.

From figures 4.12 and 4.13 the control efforts stay within the imposed constraints. The first control input, $cos(\beta)$ is needed for only 0.03 s. The second control input, v is in effect for a period of 0.09 s. This means that the control efforts in total take only 0.09 s to bring the system to an equilibrium.

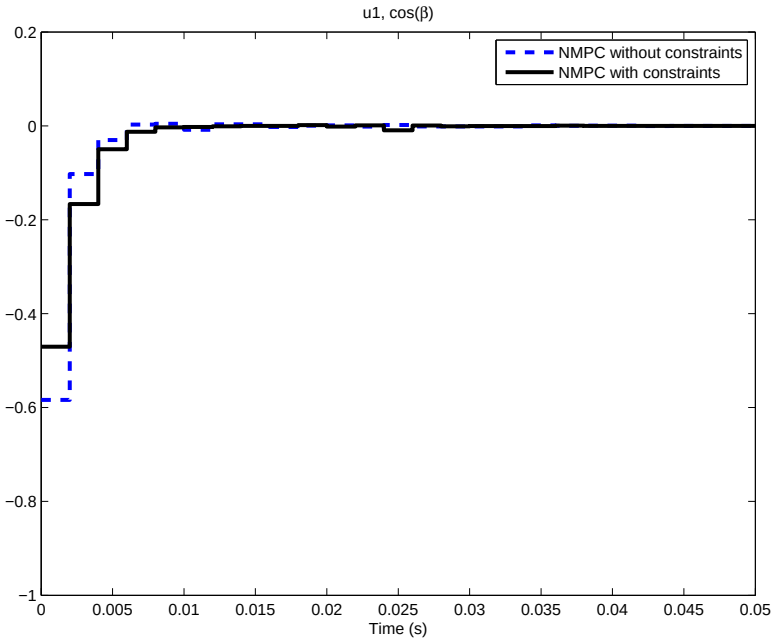

Figure 4.12: $u1$, $cos(\beta)$ Case 2.

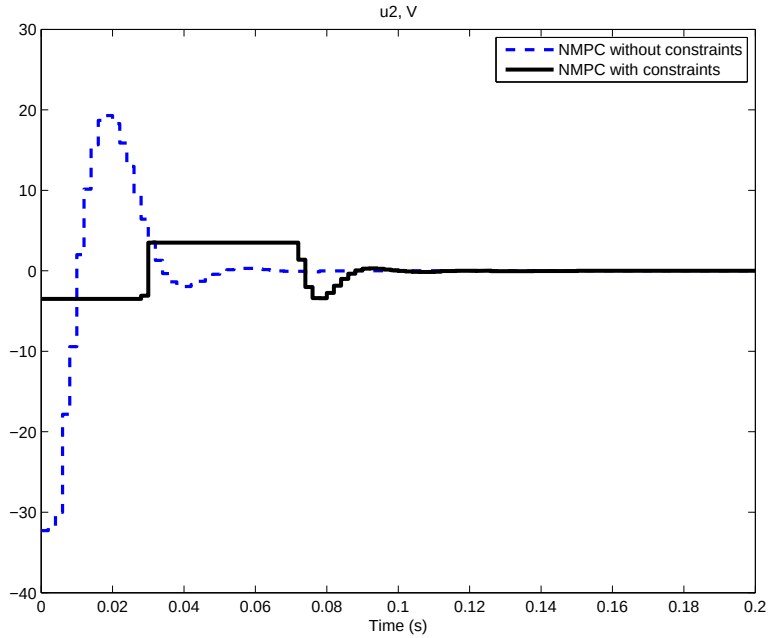

Figure 4.13: $u2$, v Case 2.

The results of this case are compared with results of the previous work [1] which used the Variable Structure Control (VSC) approach which involves the following:

1. Transforming the nonlinear state space system into a Luenberg canonical

form.

2. Constructing a suitable sliding surface.

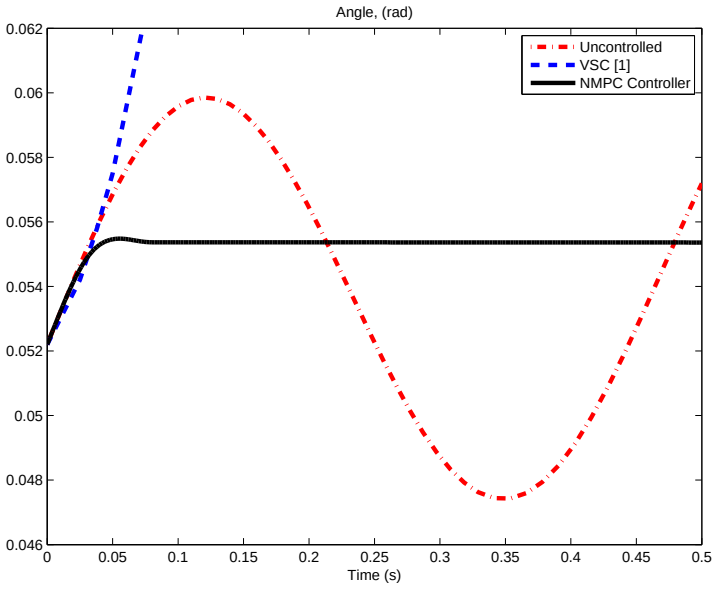

Figure 4.14: Rotor Angle comparison between VSC [1] and NMPC

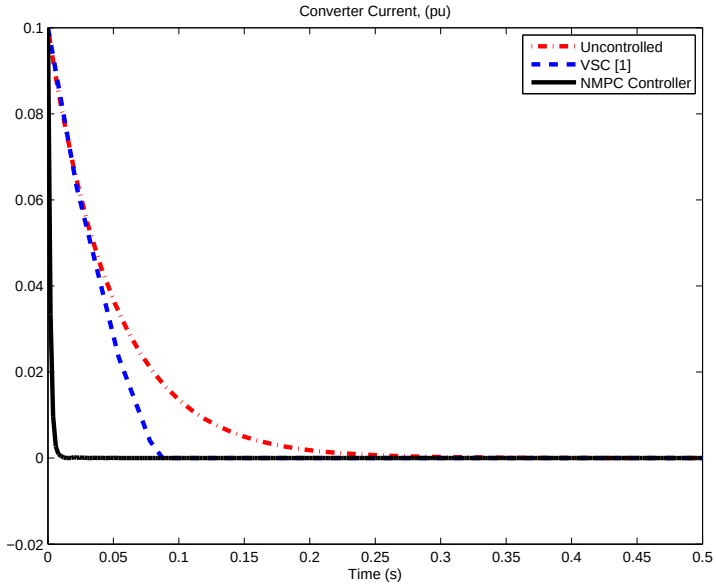

Figure 4.15: Converter Current comparison between VSC [1] and NMPC.

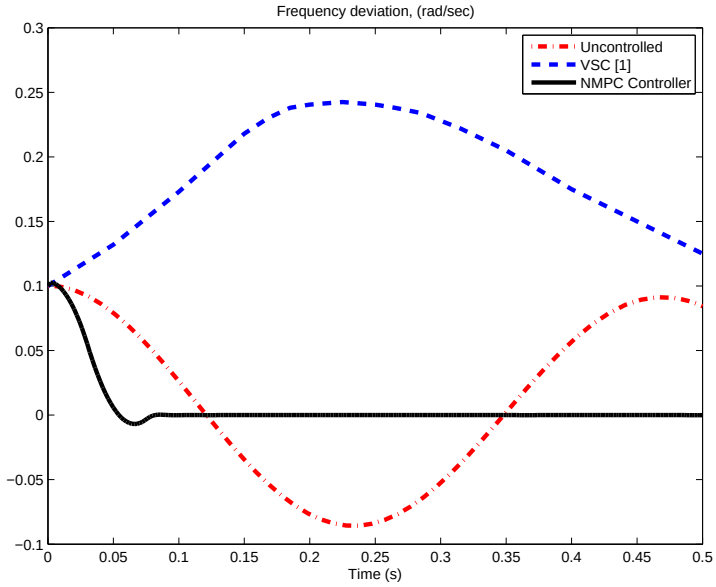

Figure 4.16: Frequency Deviation comparison between VSC [1] and NMPC.

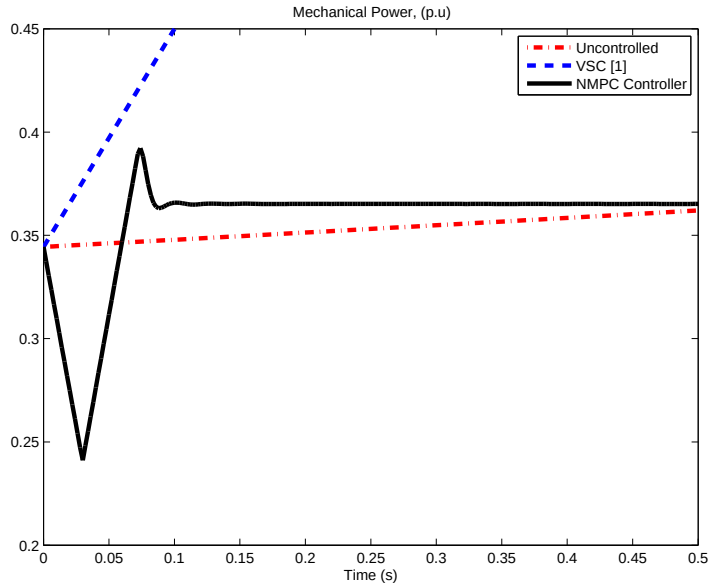

Figure 4.17: Mechanical Power comparison between VSC [1] and NMPC.

The behavior of the controlled outputs, converter current, I_d and frequency deviation, ω are seen in figures 4.15 and 4.16 respectively. The converter current with NMPC is sharply converged to equilibrium at 0.015 s compared to 0.0875 s with VSC. The frequency deviation is also settled to zero as stated in control

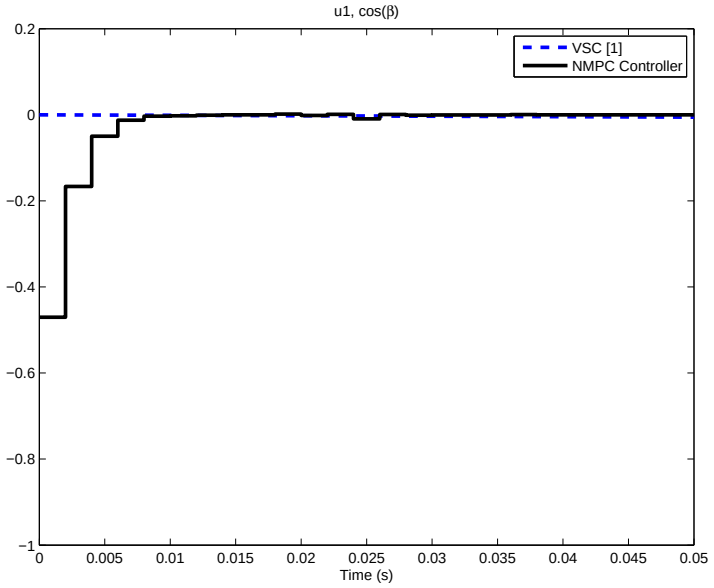

Figure 4.18: $u1$, $cos(\beta)$ comparison between VSC [1] and NMPC.

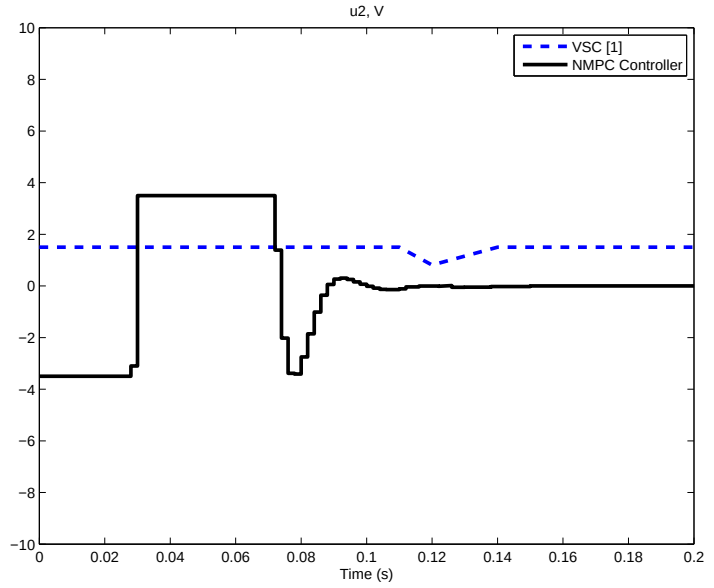

Figure 4.19: $u2$, v comparison between VSC [1] and NMPC.

goals at 0.08 s with NMPC which means that the frequency is brought to desired working frequency 60 Hz, whereas the frequency deviation with VSC takes so longer to converge. For rotor angle it is seen that NMPC doesn't make more change in the rotor angle as shown in figure 4.14 and it is settled to steady state

at value of 0.05537 rad, while in previous work the rotor angle took a higher value. The same thing applied with mechanical power, which converged to equilibrium at value of 0.3653 p.u which is lesser than with VSC. The low values of rotor angle and mechanical power in case of NMPC controller show that the machine reserved certain amount of the mechanical power.

The control efforts are shown in figures 4.18 and 4.19. The First control input, $cos(\beta)$ is needed for only 0.02 s with NMPC starting with a value of -0.4704 and then decreasing gradually to zero. The second control input, v it began with lower limit -3.5 and switched to upper limit 3.5 at 0.03 s before it converged to zero. This means that the control inputs with NMPC have tried to use the whole range of limitations to bring the system to equilibrium. The other thing which can be seen is the first input had impact on the converter current, whereas the second input had impact on the frequency deviation.

4.3.3 Case 3: Robustness of NMPC Controller

In this case the system is tested to show the robustness of the NMPC due to the parameter variations of the system. The parameter variations of the system are given by increasing the values of resistive and reactive components X, R_c, and L by 15% :

- X changed from to 0.2 p.u to 0.23 p.u.
- R_c changed from to 0.3 p.u to 0.345 p.u.

- L changed from to 0.015 p.u to 0.01725 p.u.

It is very interesting to see how the controller is able to bring the system from major variations of system's parameters to steady state.

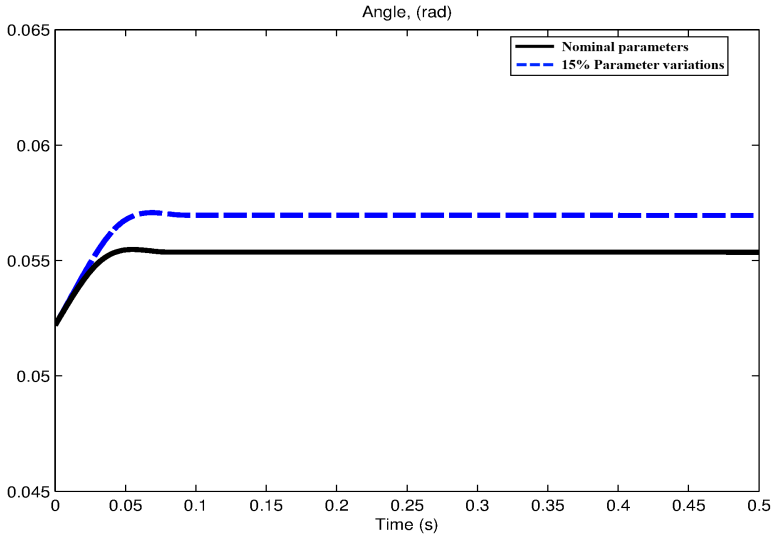

Figure 4.20: Rotor Angle Case 3

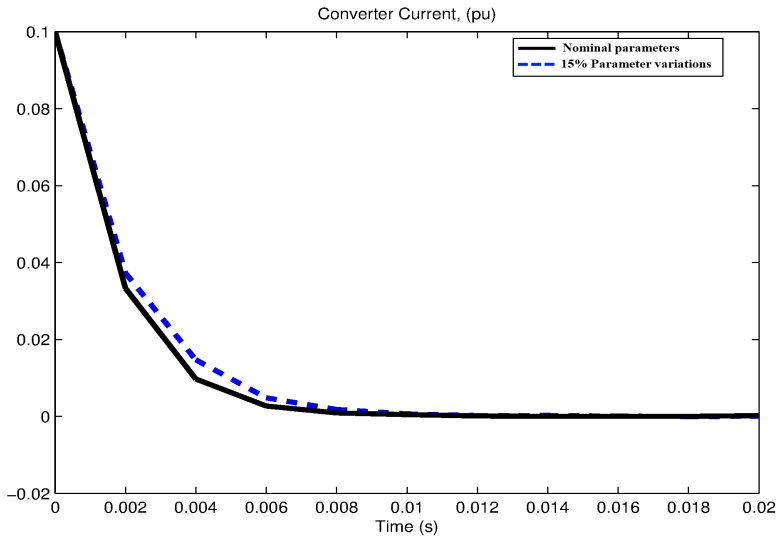

Figure 4.21: Converter Current Case 3.

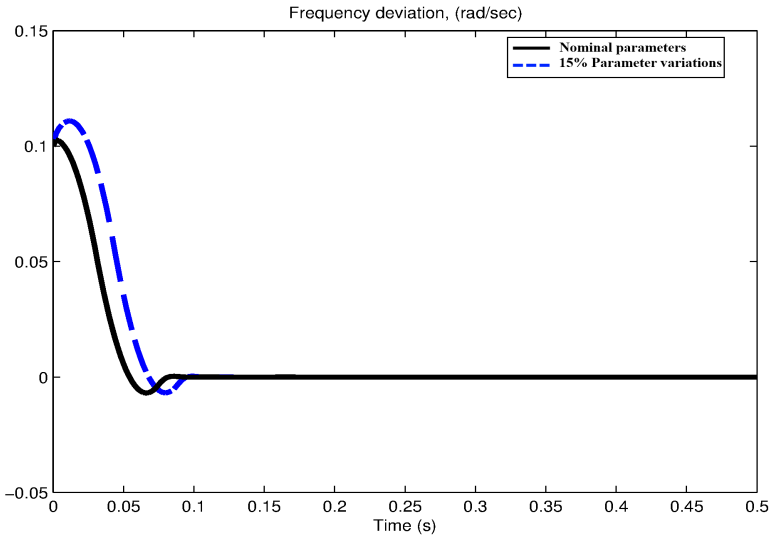

Figure 4.22: Frequency Deviation Case 3.

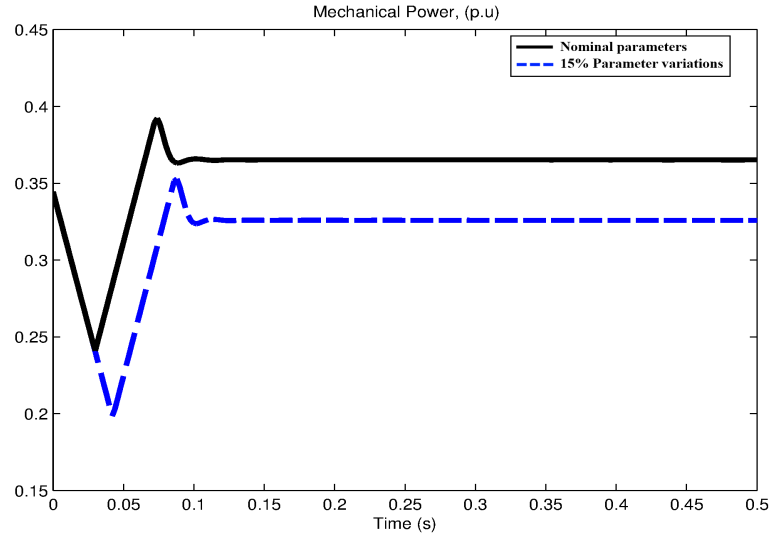

Figure 4.23: Mechanical Power Case 3.

From figures 4.8 to 4.25 it is seen that the NMPC is able to bring the system to equilibrium even with the presence of major parameter variations. The frequency deviation had a maximum value 0.1109 rad/sec with parameter variations before it smoothly went to zero in 0.106 s compared to 0.015 s with nominal parameters. The converter current settled to zero approximately at the same time with nominal

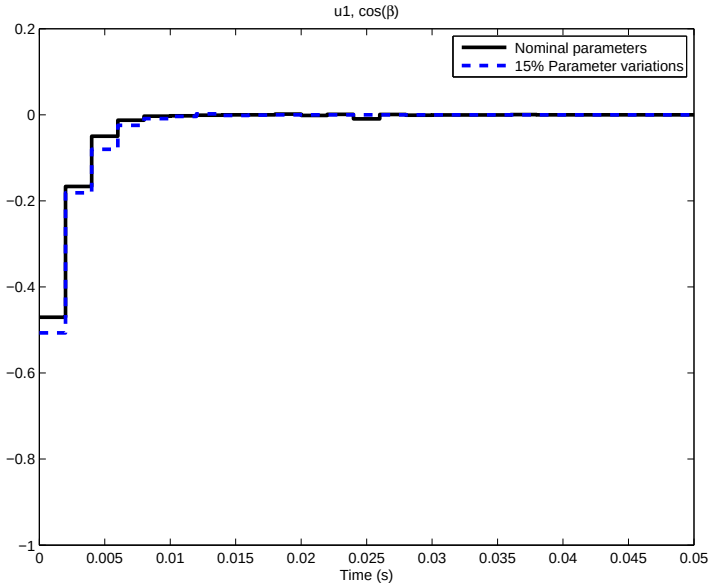

Figure 4.24: $u1$, $cos(\beta)$ Case 3.

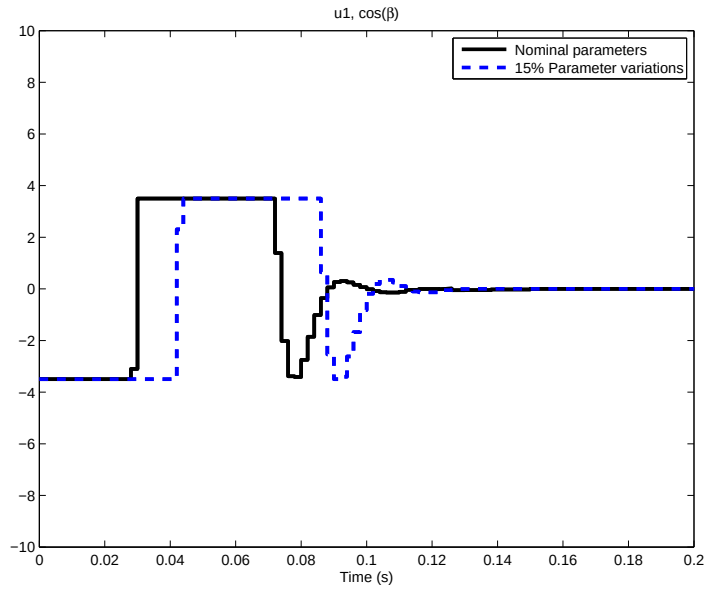

Figure 4.25: $u2$, v Case 3.

parameters. The major parameter variations led the rotor angle and mechanical power to settle to values of 0.05696 rad and 0.3259 p.u respectively, which are slightly different from nominal parameters. The controller applied a large control effort at several instants of time to drive the system to equilibrium as quickly as

possible, although, the constraints stated by equations 4.14 and 4.15 are always met.

CHAPTER 5

APPLICATION OF NONLINEAR MODEL PREDICTIVE CONTROL ON MULTI-MACHINE POWER SYSTEM

In this chapter, NMPC controller is applied to the Multi-machine Power System (MMPS). The control of MMPS is tested under different cases of large disturbances including: three phase fault, system load changing, and mechanical power change.

5.1 Design of NMPC Control for MMPS

5.1.1 3-Machines 9-bus WSCC System

The popular Western System Coordinated Council (WSCC) 3-machines 9-bus power system is selected in this thesis as a Multi-machine Power System. This system is used widely in the literature to represent the Multi-machine Power System [93]. The 3-Machines 9-bus WSCC system is shown in figure 5.1. The detailed system and machine data are listed in the Anderson and Fouad Book [93].

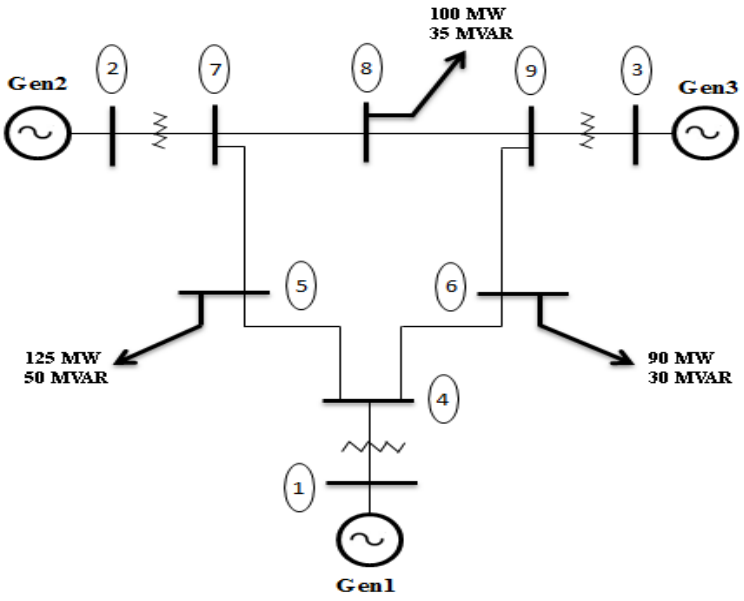

Figure 5.1: 3-Machines 9-bus WSCC system.

5.1.2 Nonlinear Model of MMPS

The Dynamics of Multi-Machine Power System is highly nonlinear and it can be represented by the third order model [2, 93, 94]:

$$\dot{\delta}_i = \omega_i - \omega_0 \tag{5.1}$$

$$\dot{\omega}_i = \frac{\omega_0}{2H}\left[P_{mi} - \frac{D_i}{\omega_0}\left[\omega_i - \omega_0\right] - P_{ei}\right] \tag{5.2}$$

$$\dot{E'_{qi}} = \frac{1}{T'_{doi}}\left[u_i - E_{qi}\right] \tag{5.3}$$

Where

$$E_{qi} = E'_{qi} + \left(x_d - x'_d\right) I_{di} \tag{5.4}$$

$$P_{ei} = \sum_{j=1}^{n} E'_{qi}\left[G_{ij}\cos\delta_{ij} + B_{ij}\sin\delta_{ij}\right] E'_{qj} \tag{5.5}$$

$$Q_{ei} = \sum_{j=1}^{n} E'_{qi}\left[G_{ij}\sin\delta_{ij} - B_{ij}\cos\delta_{ij}\right] E'_{qj} \tag{5.6}$$

$$I_{di} = -\frac{Q_{ei}}{E'_{qi}} \tag{5.7}$$

The terms used in the dynamics can be defined as follows:

δ_i: Rotor angle of ith machine in radian.

ω_i: Rotor speed of ith machine in radian/s.

ω_0: System reference speed $(2\pi f)$ in radian/s, f=60 Hz.

I_d: Stator currents in d-axis of ith machine in p.u.

P_{mi}: Input mechanical power of ith machine in p.u.

P_{ei}, Q_{ei}: Active and reactive power delivered at the terminals of ith machine in

p.u.

E'_{qi}: Internal transient voltage in q-axis of ith machine in p.u.

H_i: Inertia constant of ith machine in seconds.

D_i: Damping power coefficient of ith machine in p.u.

x_{di}, x'_{di}: Synchronous reactance and transient reactance in d-axis of ith machine in p.u.

T'_{doi}: Field winding time constant in seconds.

G_{ij}, B_{ij}: Transfer conductance and susceptance between buses i and j: respectively in p.u, where the transfer admittance $Y_{ij} = G_{ij} + jB_{ij}$.

u_i: Excitation voltage of ith machine in p.u.

With n-machine there are $3n$ differential equations. Thus, the WSCC 3-machine power system shown in figure 5.1 will have 9 differential equations. The set of nonlinear third-order differential equations 4.1, 4.2, and 5.3 can be written in the form:

$$\dot{x} = f(x, x_0, u, t) \tag{5.8}$$

where x is the state vector of dimension $(3n \times 1)$.

$$x = [\delta_1, \omega_1, E'_1 \ldots \delta_i, \omega_i, E'_{qi}] \tag{5.9}$$

5.1.3 MMPS Constraints

The excitation voltage (u_i) of ith machine, which is taken as an input control of the system has a physical limit taken as [2]:

$$-3\ p.u \leq u_i \leq 6\ p.u \tag{5.10}$$

5.1.4 Operating Condition

In order to reduce the complexity of the transient stability analysis, some simplifying assumptions are made as follows [93, 94, 95]:

1. There is no loss of power in lines.

2. Mechanical Power assumed constant during transient.

3. All system data are converted to a common base: a system base of 100 MVA is frequently used.

4. Obtain the initial values from the load-flow study for pre-transient case. Usually the generator armature resistances are neglected.

5. Loads in the system are converted to equivalent admittances.

6. Construct the admittance matrix or what is called Y-matrix which includes the admittances between buses, admittance of converted loads, and the admittance of internal generator impedances.

Bus	Voltage	Angle	Load		Generation		Injected
No.	(p.u)	(deg)	MW	MVar	MW	MVar	MVar
1	1.040	0.0	0	0	71.594	27.032	0
2	1.025	9.279	0	0	163.0	6.657	0
3	1.025	4.664	0	0	85.0	−10.856	0
4	1.026	−2.217	0	0	0	0	0
5	0.996	−3.989	125	50	0	0	0
6	1.013	−3.688	90	30	0	0	0
7	1.026	3.719	0	0	0	0	0
8	1.016	0.727	100	35	0	0	0
9	1.032	1.966	0	0	0	0	0
Total			315.0	115.0	319.954	22.833	

Table 5.1: Load flow results

7. Finally, obtain the reduced Y-matrix by eliminating all nodes except the internal generator nodes. The final system diagram is shown in figure 5.2.

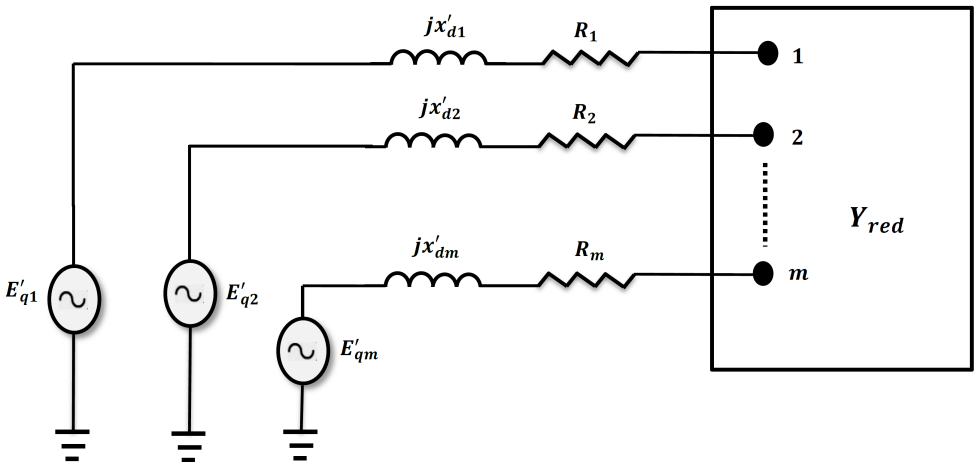

Figure 5.2: Reduced Network of MMPS.

The operating conditions of MMPS are found by applying the load flow data of the considered system using conventional fast-decoupled method. More details about load flow and conventional fast-decoupled method can be found in [96]. The load flow data is shown in table 5.1.

5.1.5 Control Objective

The control objective is to maintain the stability of MMPS after being subjected to large disturbances, such as three phase fault, load change, and mechanical power change.

In order to determine the stability of the system, it is expected that the difference between the rotor angle of the reference machine which is in this case machine-1 and the angles of other machines reaches a maximum value and then deceases. Another indication of stability is that the difference between machine speeds with respect to the reference machine-1 should equal zero.

5.1.6 Proposed Cost Function

The desired cost function of NMPC controller to achieve the control objective is proposed as:

$$J = \sum_{k=0}^{N-1} (\omega_i(k) - \omega_0)^2 \tag{5.11}$$

where

N: The Prediction Horizon.

ω_0: System reference speed ($2\pi f$) in radian/s, f=60 Hz.

It is well known that the complexity of simulation and the design of controller depend on many factors, such as prediction horizon (N) and sampling time (Δt). Different values of N and Δt have been tried and compromised values were found to be $N = 0.5$ s and $\Delta t = 0.01$ s, for all cases of simulation (three phase fault,

load change, and mechanical power change). Also for comparison purpose the damping power coefficient D=0 for the three machines. The operating frequency f=60 Hz.

As stated in section (3.3) the active set algorithm is selected to solve the optimization problem using function "fmincon" from MATLAB® Optimization Toolbox.

5.2 Three Phase Fault

In this section, a three phase fault is applied in two different places of 3-Machines 9-bus WSCC system.

5.2.1 Three Phase Fault near Bus-7

The transient is initiated by applying a three phase fault near bus-7 at the end of line 5-7 at time equal 1 s. The fault is cleared in five cycles (0.083 s) by fast relays opening the line 5-7, where the system is in steady state before 1 s.

In order to study the system performance when subjected to an abnormal conditions (such as a fault), the system configurations post the fault, during the fault and after fault have to be determined. Therefore,the transfer admittance matrix

before fault (Y_{bf}), during fault (Y_{df}), and after fault (Y_{af}) are given as follows:

$$Y_{bf} = \begin{bmatrix} 0.8455 - 2.9882i & 0.2871 + 1.5129i & 0.2096 + 1.2256i \\ 0.2871 + 1.5129i & 0.4199 - 2.7238i & 0.2132 + 1.0879i \\ 0.2096 + 1.2256i & 0.2132 + 1.0879i & 0.2770 - 2.3681i \end{bmatrix} \tag{5.12}$$

$$Y_{df} = \begin{bmatrix} 0.6568 - 3.8160i & 0.0000 + 0.0000i & 0.0701 + 0.6305i \\ 0.0000 + 0.0000i & 0.0000 - 5.4854i & 0.0000 + 0.0000i \\ 0.2096 + 1.2256i & 0.0000 + 0.0000i & 0.1740 - 2.7959i \end{bmatrix} \tag{5.13}$$

$$Y_{af} = \begin{bmatrix} 1.1386 - 2.2965i & 0.1290 + 0.7063i & 0.1823 + 1.0637i \\ 0.1290 + 0.7063i & 0.3744 - 2.0150i & 0.1921 + 1.2066i \\ 0.1823 + 1.0637i & 0.1921 + 1.2066i & 0.2691 - 2.3516i \end{bmatrix} \tag{5.14}$$

To investigate the effectiveness of the proposed controller the results of this case are compared with results reported in literature [2] which used the state feedback control scheme based on the Standard Linearization Technique (SLT) which involves the following:

1. Construct the state space of the system. Define the place of the fault time of occurrence of the fault, and clearing time of the fault.

2. Obtain the state feedback linear gains using linear optimal control strategy.

3. Compute Δu_i at every iteration by substituting the state variables.

4. Update the control input u_i at the end of each iteration by $u_i = u_i + \Delta u_i$ and use it in the next iteration.

5. Repeat steps 3 and 4 till final simulation time is attained.

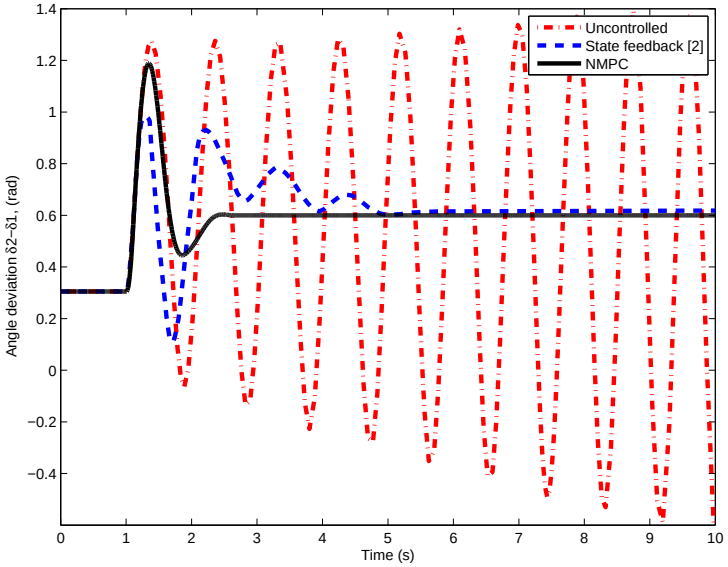

Figure 5.3: Angle deviation $(\delta_2 - \delta_1)$ of fault near bus-7.

Simulation Results

Figures 5.3, 5.4, 5.5, and 5.6 show the response of the system, where the dash-dot line, dashed line, and solid line are uncontrolled, state feedback, and NMPC respectively.

As can be seen, the angle deviations $(\delta_2 - \delta_1)$ and $(\delta_3 - \delta_1)$ in figures 5.3 and 5.4 reached the steady state after being disturbed by the three phase fault. With NMPC, both angle deviations $(\delta_2 - \delta_1)$ and $(\delta_3 - \delta_1)$ are brought to steady state

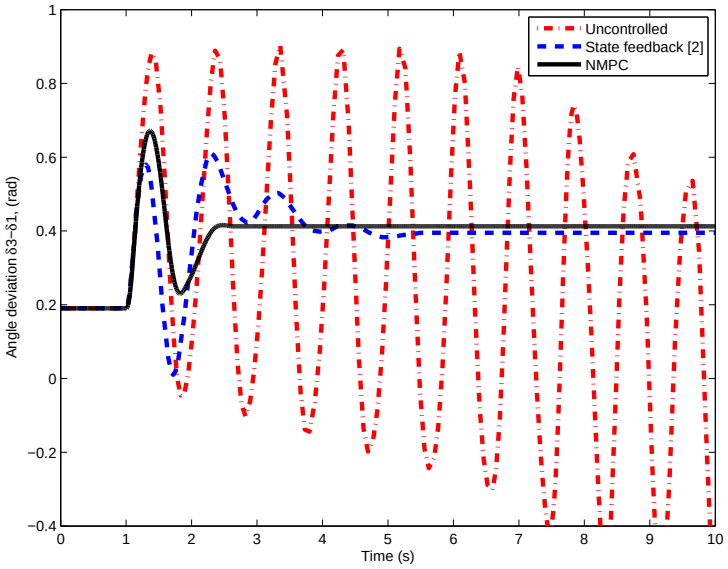

Figure 5.4: Angle deviation $(\delta_3 - \delta_1)$ of fault near bus-7.

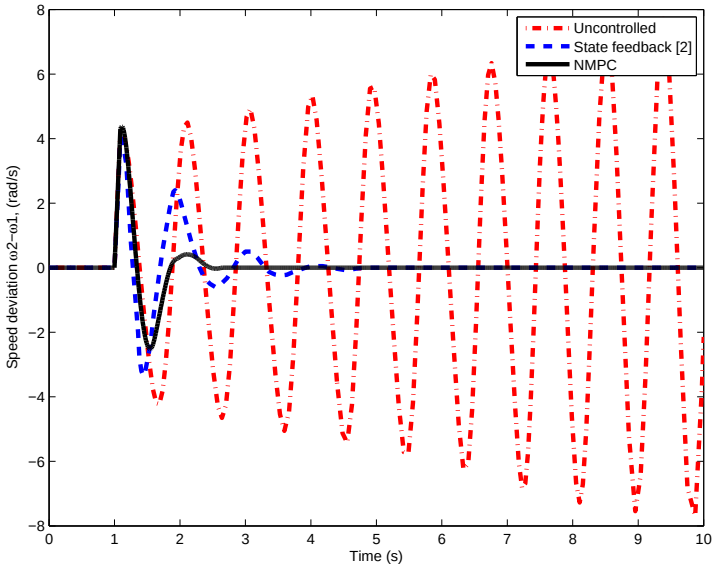

Figure 5.5: Speed deviation $(\omega_2 - \omega_1)$ of fault near bus-7.

at 2.62 s, whereas with state feedback [2] the angle deviations reached the steady state at approximately 5 s, which is almost double the time needed by proposed NMPC controller. The steady state values of angle deviations $(\delta_2 - \delta_1)$ and $(\delta_3 - \delta_1)$ are 0.5992 rad and 0.412 rad respectively.

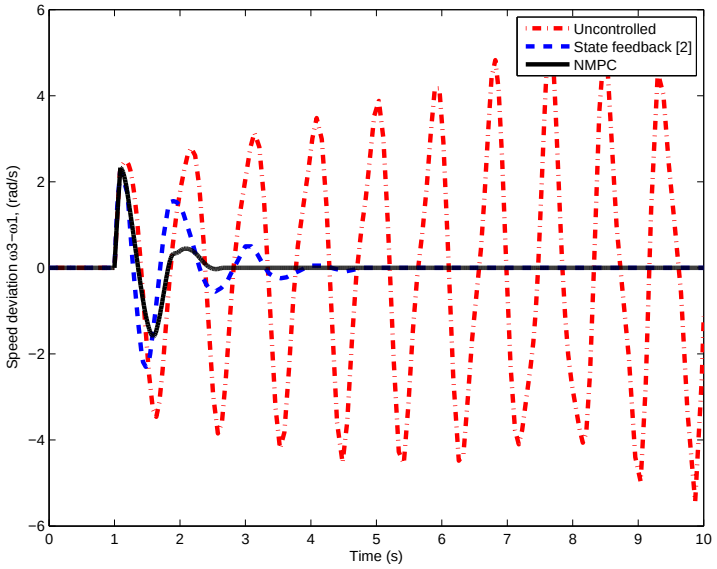

Figure 5.6: Speed deviation $(\omega_3 - \omega_1)$ of fault near bus-7.

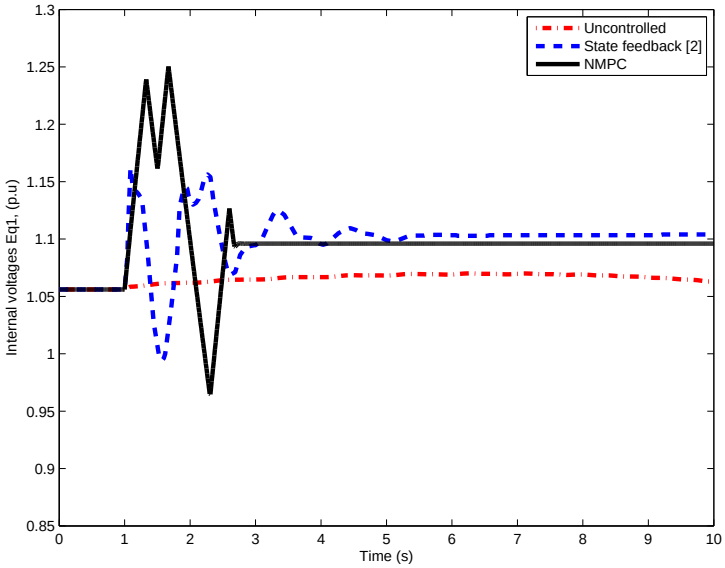

Figure 5.7: Internal voltage in q-axis (Eq_1) of fault near bus-7.

With NMPC controller, the speed deviations $(\omega_2 - \omega_1)$ and $(\omega_3 - \omega_1)$ converged to zero at 2.7 s compared to 5 s with state feedback controller [2]. This means that the control objective is achieved by NMPC controller, and consequently, the system frequency is brought to 60 Hz at 2.7 s after the fault is cleared. Another feature can be noticed from the system response is that the NMPC controller

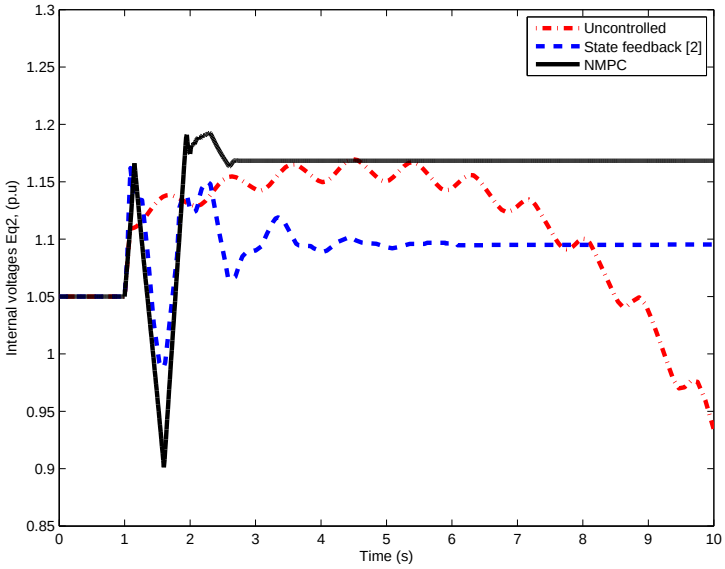

Figure 5.8: Internal voltage in q-axis (Eq_2) of fault near bus-7.

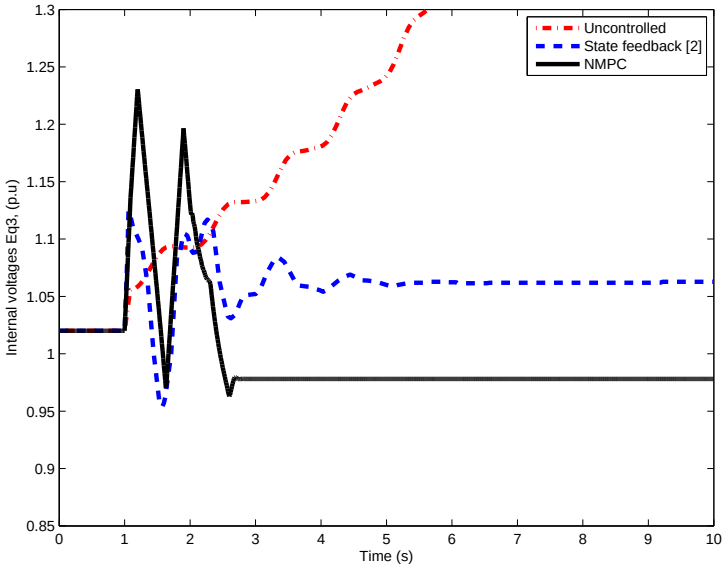

Figure 5.9: Internal voltage in q-axis (Eq_3) of fault near bus-7.

provides a superior damping in comparison with the state feedback controller [2].

The internal voltages in q-axis of the three machines, Eq_1,Eq_2, and Eq_3 are shown in figures 5.7, 5.8, and 5.9 respectively. The results with NMPC controller demonstrated that these voltages settled to steady state values, 1.095 p.u, 1.168

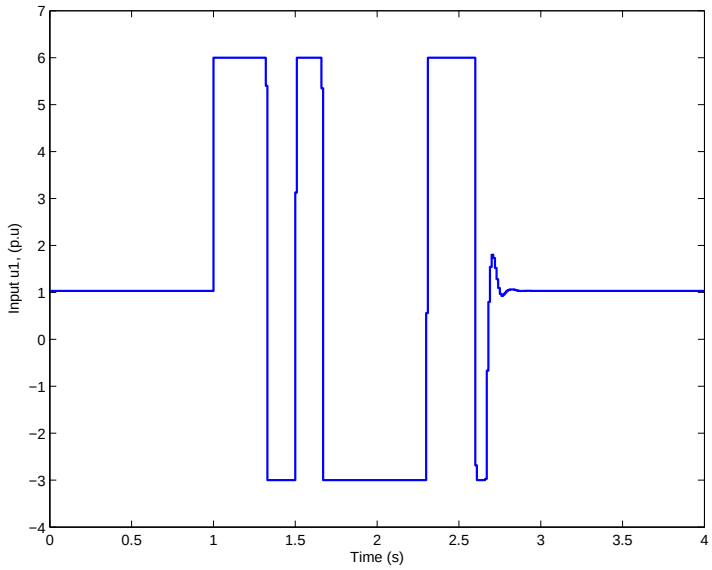

Figure 5.10: Input, u_1 of fault near bus-7.

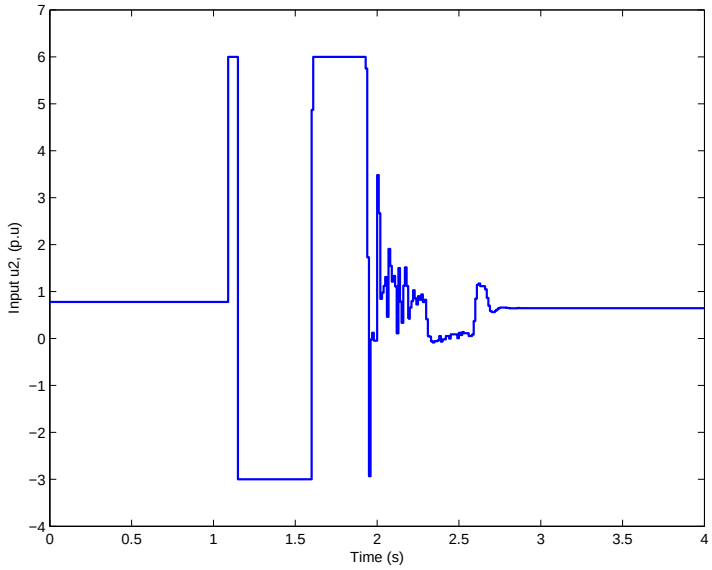

Figure 5.11: Input, u_2 of fault near bus-7.

p.u and 0.978 p.u respectively.

Again the figures demonstrated that the present NMPC controller outperforms the method in [2] in terms of settling time and damping of the first swing oscillation.

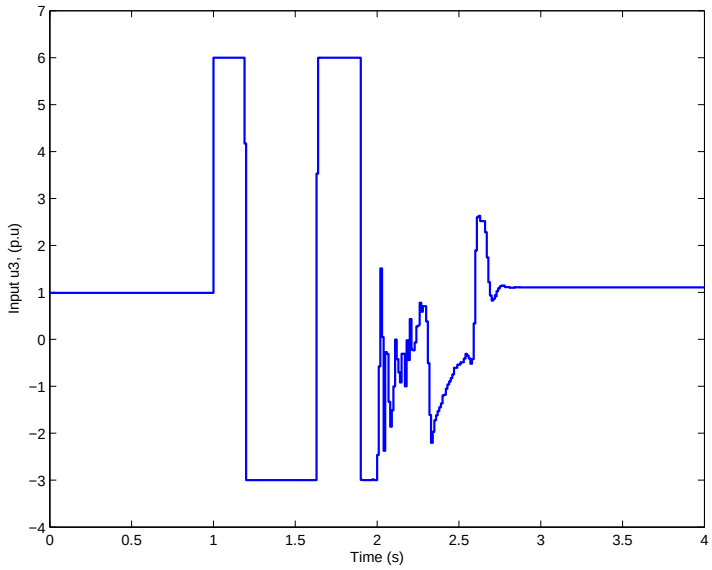

Figure 5.12: Input, u_3 of fault near bus-7.

The three control efforts (excitation voltages) u_1, u_2 and u_3 are shown in figures 5.10,5.11, and 5.12 respectively. The NMPC controller applied large control efforts in order to bring the system to equilibrium as quickly as possible. It is seen that the three inputs are stayed within the constraints $(-3 \leq u_i \leq 6)$ as stated in equation 5.10.

5.2.2 Three Phase Fault near Bus-8

This case is considered to test the ability of NMPC controller to bring the system to steady state even when the fault place is changed. In this case the transient is initiated by applying a three phase fault near bus-8 at the end of line 8-9 at time equals 1 s. The fault is cleared in five cycles (0.083 s) by tripping the line 8-9, where the system is in steady state before 1 s.

The assigned values of the transfer admittance matrix Y_{ij} for the three conditions (post-fault, during fault, and after fault) are given below:

$$Y_{bf} = \ matrix \ (5.12) \tag{5.15}$$

$$Y_{df} = \begin{bmatrix} 0.6850 - 3.6849i & 0.0769 + 0.5228i & 0.0504 + 0.4984i \\ 0.0769 + 0.5228i & 0.1465 - 4.1304i & 0.0057 + 0.0547i \\ 0.0504 + 0.4984i & 0.0057 + 0.0547i & 0.1196 - 3.1270i \end{bmatrix} \tag{5.16}$$

$$Y_{af} = \begin{bmatrix} 0.8244 - 2.9998i & 0.3248 + 1.4003i & 0.1380 + 1.2933i \\ 0.3248 + 1.4003i & 0.6690 - 2.0785i & 0.0621 + 0.3337i \\ 0.1380 + 1.2933i & 0.0621 + 0.3337i & 0.2791 - 1.6186i \end{bmatrix} \tag{5.17}$$

Simulation Results

In this case, the angle deviations $(\delta_2 - \delta_1)$ and $(\delta_3 - \delta_1)$ in figures 5.13 and 5.14 fluctuated before they were brought to steady state at 2.8 s. The steady state values of angle deviations $(\delta_2 - \delta_1)$ and $(\delta_3 - \delta_1)$ are 0.126 rad and 0.16 rad respectively which are less than the initial values.

The speed deviations $(\omega_2 - \omega_1)$ and $(\omega_3 - \omega_1)$ had little fluctuations before they converged to zero at 2.88 s. This means that the control objective is achieved by

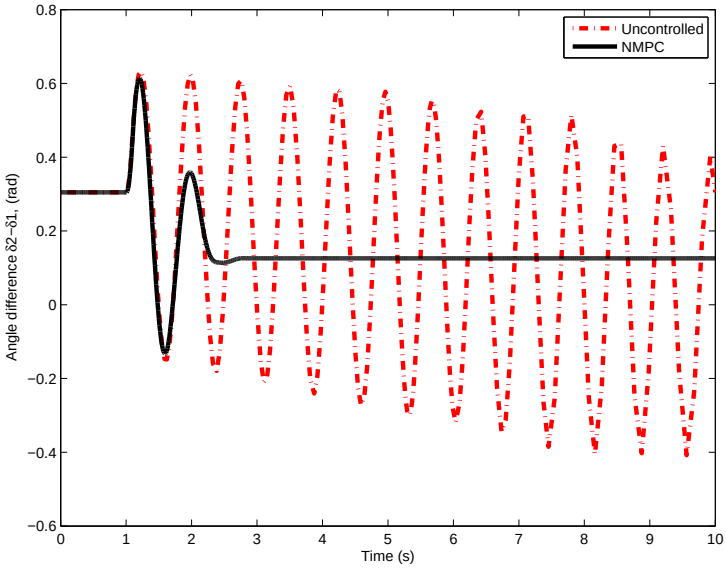

Figure 5.13: Angle deviation ($\delta_2 - \delta_1$) of fault near bus-8.

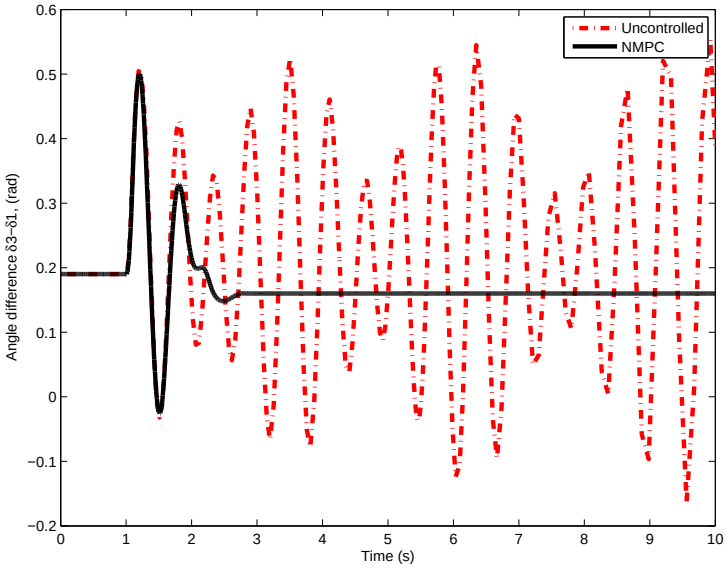

Figure 5.14: Angle deviation ($\delta_3 - \delta_1$) of fault near bus-8.

NMPC controller. However, the place of fault is changed.

From the two cases of the three phase fault, it is seen that, although the fault place is changed in the MMPS, the NMPC controller showed a good performance to bring the system to the steady state as shown in figures 5.17 and 5.18. In the

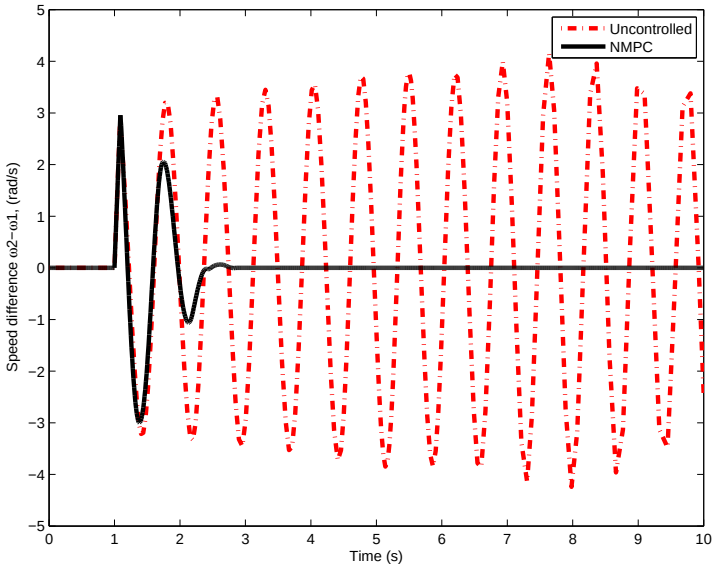

Figure 5.15: Speed deviation $(\omega_2 - \omega_1)$ of fault near bus-8.

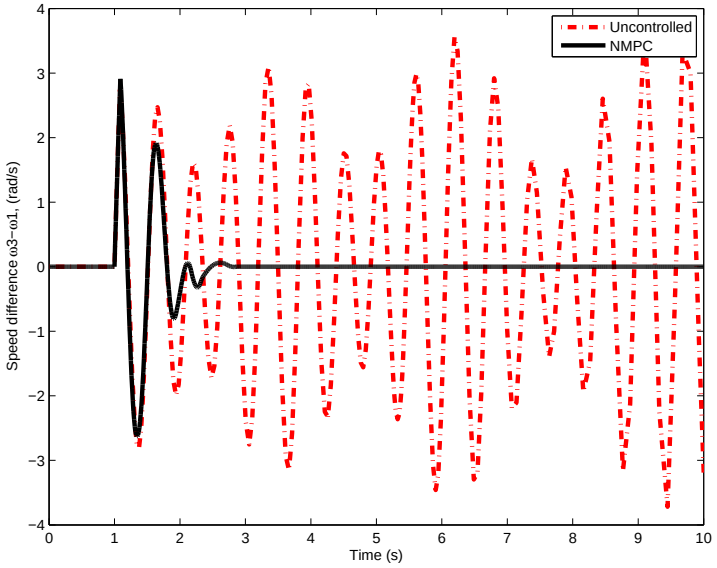

Figure 5.16: Speed deviation $(\omega_3 - \omega_1)$ of fault near bus-8.

first case when the three phase fault occurred near bus-7, the frequency deviations of MMPS are brought to steady state a little faster (2.7 s) than in the second case when the three phase fault occurred near bus-8 (2.88 s). This means that a fault at bus-8 is more critical than the fault at bus-7. Also it can be seen that in case of the three phase fault occurring near bus-8, the damping is less than that where

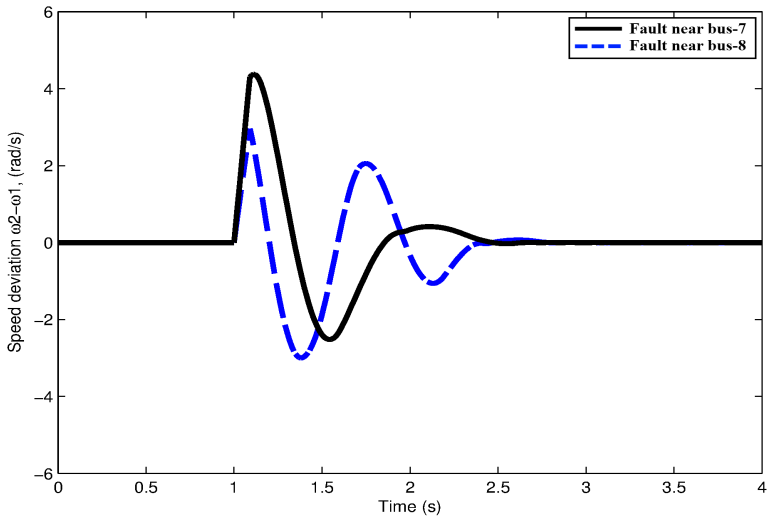

Figure 5.17: Speed deviation $(\omega_2 - \omega_1)$ of faults near bus-7 and bus-8.

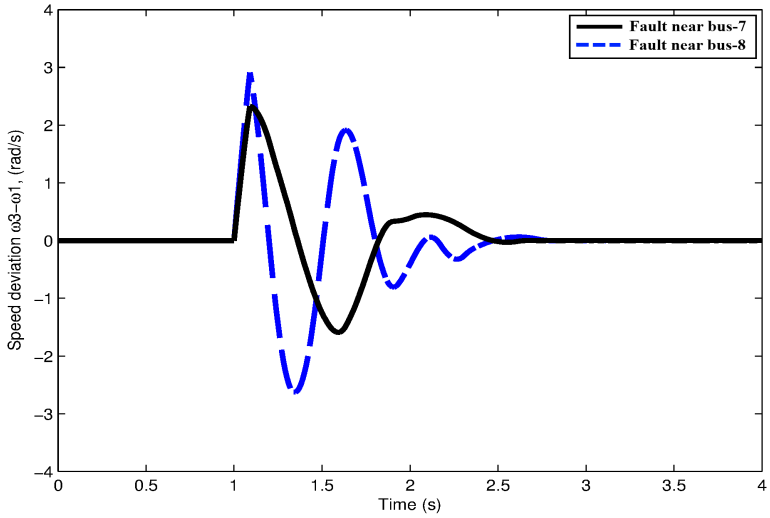

Figure 5.18: Speed deviation $(\omega_3 - \omega_1)$ of faults near bus-7 and bus-8.

the fault occurring near bus-7.

5.2.3 Robustness of NMPC Controller

The system is tested to show the robustness of the NMPC controller due to the parameter variations of the system in the case of three phase fault near bus-7.

The parameter variations of the system are given by increasing the values of resistive and reactive components of the transmission line 6-9, and the transformers between 2-7 and 3-9 by 5%.

Simulation Results

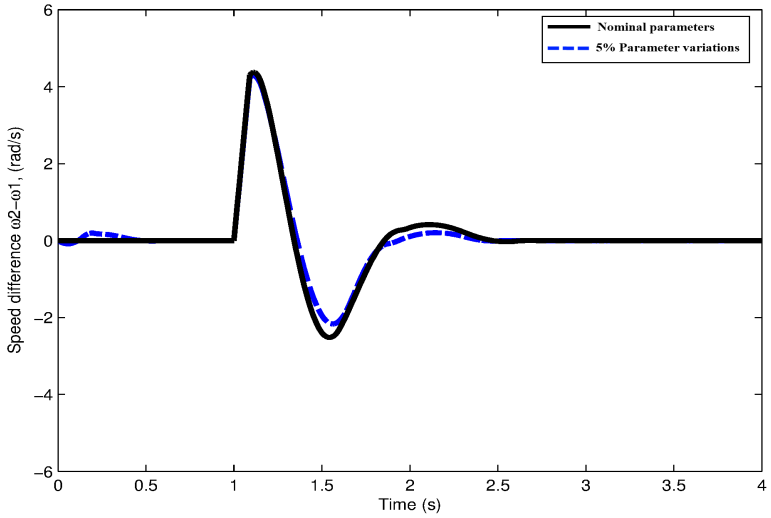

Figure 5.19: Speed deviation $(\omega_2 - \omega_1)$ of the Robustness of NMPC Controller.

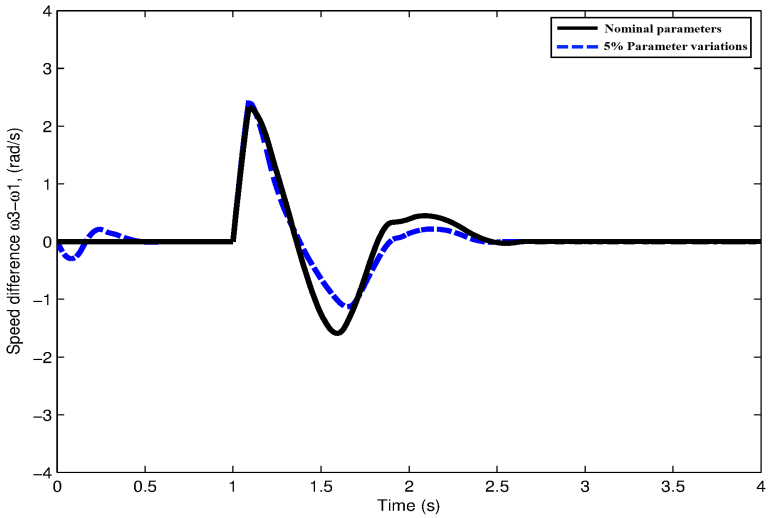

Figure 5.20: Speed deviation $(\omega_3 - \omega_1)$ of the Robustness of NMPC Controller.

From figures 5.19 and 5.19, it is seen that the NMPC controller is able to bring the system to the steady state even with the presence of parameter variations. Both frequency deviations $(\omega_2 - \omega_1)$ and $(\omega_3 - \omega_1)$ are settled to zero at 0.65 s. When the system subjected to the three phase fault at 1 s and the line is clear at five cycles the NMPC controller is still capable to bring the system to the steady state.

5.2.4 Real-time Optimization Complexity

The power processes are considered as fast processes compared to the chemical processes, thus, the time response of the power process is considered to be small. The real-time optimization complexity of proposed framework of control is restricted by the following factors:

1. Complexity of the system: with more machines the computation will increase due to more effort to be made to solve the differential equations.

2. Sampling time: as long as the process is fast, only a small sampling time is necessary. This means more computation to be performed in each step.

3. Prediction horizon: despite the increase in the prediction horizon giving a good view of the process's future, it increases the load on the optimization process.

4. Constraints: constraints are involved in the optimization process and should be satisfied.

Δt (s)	N (s)	Computational time (s/sample)
0.01	0.7	22
0.01	0.5	9
0.01	0.3	5
0.005	0.5	17
0.015	0.5	113

Table 5.2: Computational time

In the present work, the computational time is approximately equals to 9 s per sample for a case of three phase fault near bus-7 with sampling time equal 0.01 s, prediction horizon 0.5 s, and with constraints imposed in 5.10. This simulation is run on MATLAB® with an Intel Core i5 CPU @2.53GHz with 6GB of RAM. Table listed the computational time for different values of sampling time (Δt) and prediction horizon (N).

This computation time can be improved to make the implementation in real-time possible by using high speed processors or by using other fast techniques of optimization.

5.3 System Load Changing

Another scenario to examine the performance of NMPC controller is by changing the MMPS's loads. In this section, a 50% step change, increasing or decreasing, has been applied to the three load buses (5, 6, and 8) at time of 1 s. Table 5.3 shows the values of the changing of load buses.

Bus	50% Load Increase		Nominal Load		50% Load Decrease	
No.	MW	MVar	MW	MVar	MW	MVar
5	187.5	75	125	50	62.5	25
6	135	45	90	30	45	15
8	150	52.5	100	35	50	17.5

Table 5.3: Load changes.

5.3.1 Load Changing of Bus-5

The load in bus-5 is changed by 50%, increasing and decreasing, as shown in table 5.3. This change occurred at 1 s. The change in load is reflected on the transfer admittance matrix Y_{ij}, which will change from its nominal values. The transfer admittance matrix when the load is increased by 50% is $Y_{loadincrease}$ and when decreased is $Y_{loaddecrease}$. The values are:

$$Y_{loadincrease} = \begin{bmatrix} 0.9724 - 3.8160i & 0.3605 + 1.4204i & 0.2506 + 1.1713i \\ 0.3605 + 1.4204i & 0.4630 - 2.7751i & 0.2374 + 1.0577i \\ 0.2506 + 1.1713i & 0.2374 + 1.0577i & 0.2907 - 2.3860i \end{bmatrix} \quad (5.18)$$

$$Y_{loaddecrease} = \begin{bmatrix} 0.7039 - 2.8456i & 0.2058 + 1.5907i & 0.1641 + 1.2713i \\ 0.2058 + 1.5907i & 0.3728 - 2.6810i & 0.1868 + 1.1132i \\ 0.1641 + 1.2713i & 0.1868 + 1.1132i & 0.2620 - 2.3531i \end{bmatrix} \quad (5.19)$$

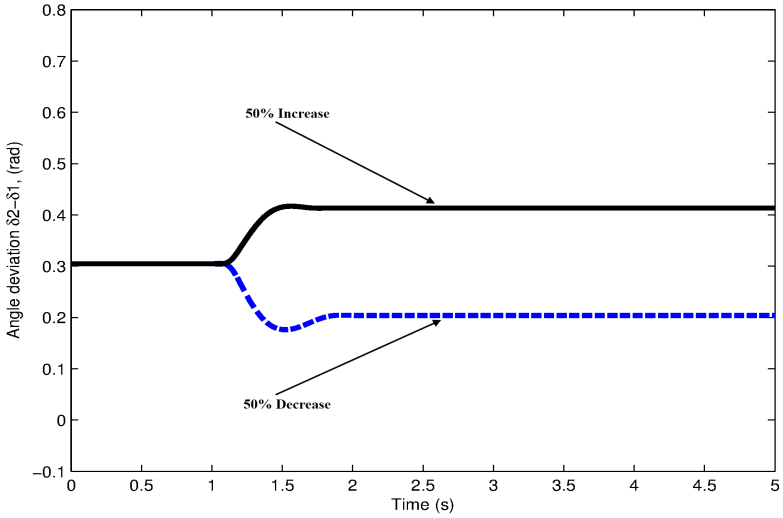

Figure 5.21: Angle deviation $(\delta_2 - \delta_1)$ of load change bus-5.

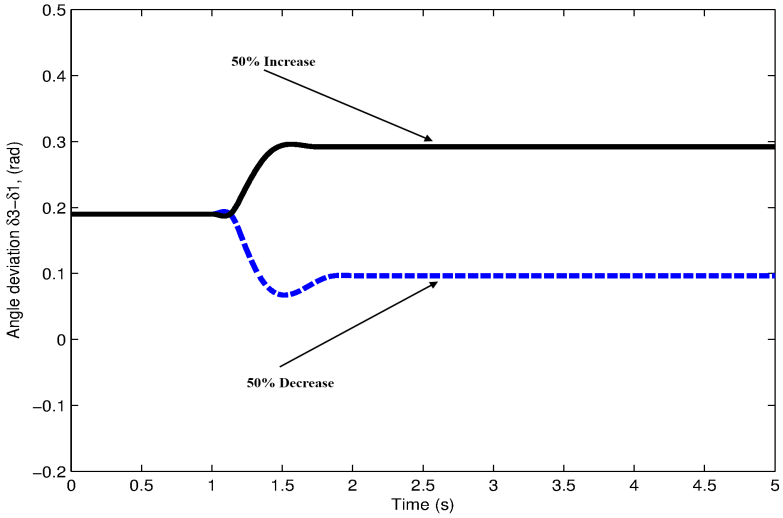

Figure 5.22: Angle deviation $(\delta_3 - \delta_1)$ of load change bus-5.

Simulation Results

Figures 5.21 and 5.22 show the system response of both cases of 50% increasing and decreasing in bus-5 load. From the response of angle deviations $(\delta_2 - \delta_1)$ and $(\delta_3 - \delta_1)$, it is shown that with increasing and decreasing the load by 50% on bus-5, the system is settled to the steady state at 1.7 s and 1.9 s respectively. The

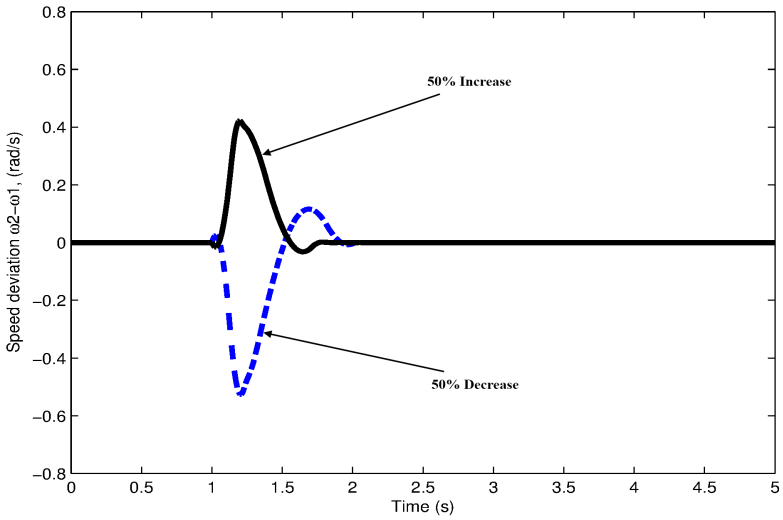

Figure 5.23: Speed deviation $(\omega_2 - \omega_1)$ of load change bus-5.

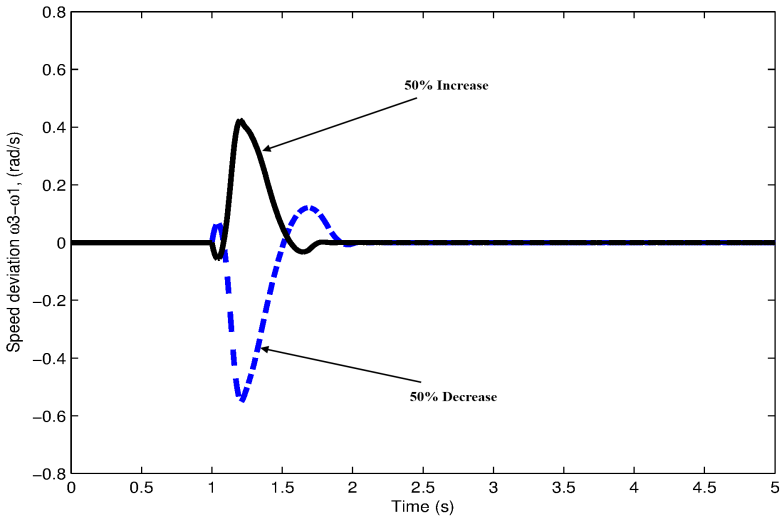

Figure 5.24: Speed deviation $(\omega_3 - \omega_1)$ of load change bus-5.

angle deviations $(\delta_2 - \delta_1)$ and $(\delta_3 - \delta_1)$ are brought to the the new steady state values 0.413 rad and 0.292 rad when the load increased by 50% and to the values 0.204 rad and 0.096 rad when the load decreased by 50%.

In addition, the speed deviations $(\omega_2 - \omega_1)$ and $(\omega_3 - \omega_1)$ of MMPS shown in figures 5.23 and 5.24 are brought to zero at 1.82 s when the load increased by 50% and 2.05 s when the load decreased by 50%.

5.3.2 Load Changing of Bus-6

In this case, the load in bus-6 is changed by 50% increasing and decreasing as shown in table 5.3. The change of load is occurred at 1 s. The transfer admittance matrix when the load is increased by 50% is $Y_{loadincrease}$ and when decreased is $Y_{loaddecrease}$. The values are:

$$Y_{loadincrease} = \begin{bmatrix} 0.9444 - 3.0911i & 0.3264 + 1.4701i & 0.2566 + 1.1782i \\ 0.3264 + 1.4701i & 0.4361 - 2.7420i & 0.2321 + 1.0680i \\ 0.2566 + 1.1782i & 0.2321 + 1.0680i & 0.2995 - 2.3901i \end{bmatrix} \quad (5.20)$$

$$Y_{loaddecrease} = \begin{bmatrix} 0.7402 - 2.8990i & 0.2452 + 1.5500i & 0.1596 + 1.2666i \\ 0.2452 + 1.5500i & 0.4029 - 2.7080i & 0.1932 + 1.1051i \\ 0.1596 + 1.2666i & 0.1932 + 1.1051i & 0.2531 - 2.3491i \end{bmatrix} \quad (5.21)$$

Simulation Results

Figures 5.25 and 5.26 show the system response increasing and decreasing in the load of bus-6 by 50%. The response of angle deviations $(\delta_2 - \delta_1)$ and $(\delta_3 - \delta_1)$

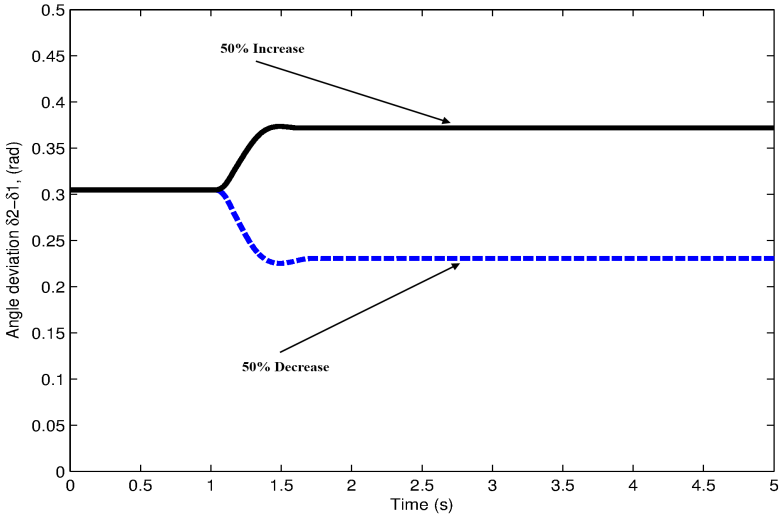

Figure 5.25: Angle deviation $(\delta_2 - \delta_1)$ of load change bus-6.

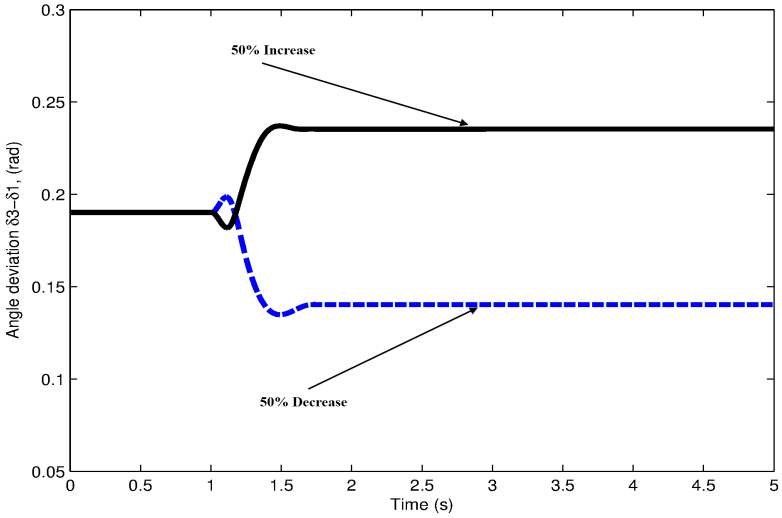

Figure 5.26: Angle deviation $(\delta_3 - \delta_1)$ of load change bus-6.

showed that with an increase and decrease of 50% in the load on bus-6, the system is settled to the steady state at 1.57 s and 1.7 s respectively. The angle deviations $(\delta_2 - \delta_1)$ and $(\delta_3 - \delta_1)$ are brought to the new steady state values 0.37 rad and 0.23 rad when the load increased by 50% and to the values 0.23 rad and 0.14 rad when the load decreased by 50%.

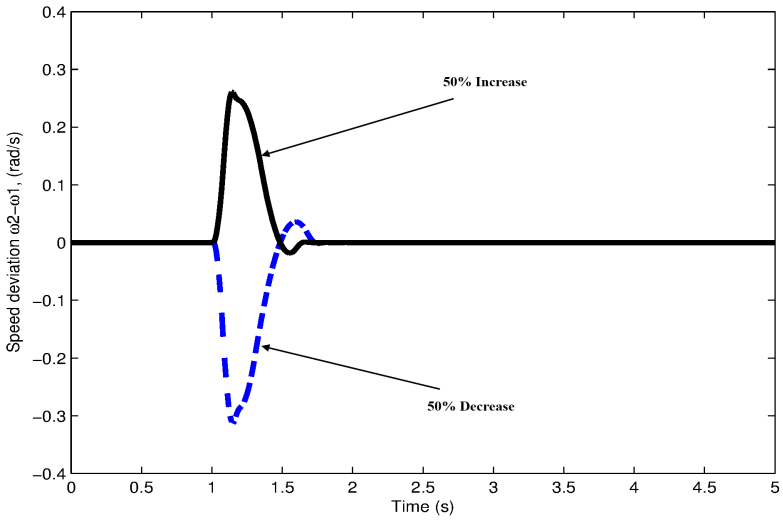

Figure 5.27: Speed deviation $(\omega_2 - \omega_1)$ of load change bus-6.

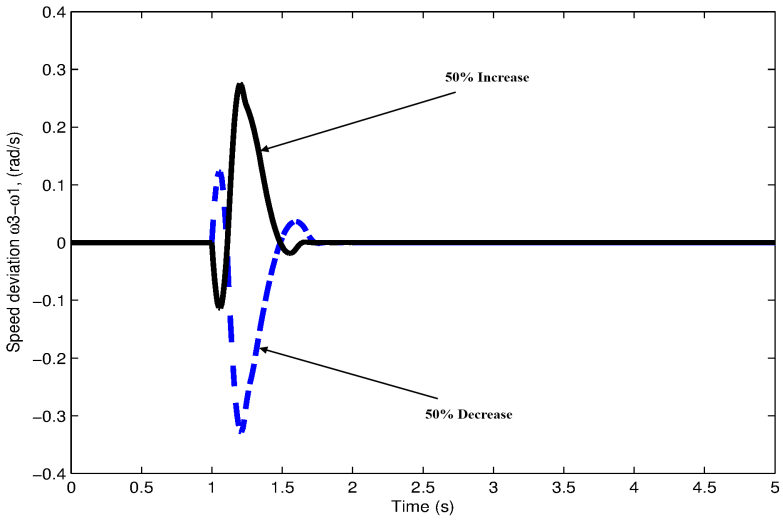

Figure 5.28: Speed deviation $(\omega_3 - \omega_1)$ of load change bus-6.

The speed deviations $(\omega_2 - \omega_1)$ and $(\omega_3 - \omega_1)$ of MMPS are brought to zero at 1.65 s when the load increased by 50% and 1.74 s when the load decreased by 50%.

5.3.3 Load Changing of Bus-8

The load in bus-8 is changed by 50% increasing and decreasing as shown in table 5.3. The change of load occurred at 1 s. The transfer admittance matrix when the load is increased by 50% is $Y_{loadincrease}$ and when decreased is $Y_{loaddecrease}$. The values are:

$$Y_{loadincrease} = \begin{bmatrix} 0.8757 - 3.0212i & 0.3305 + 1.4671i & 0.2414 + 1.1917i \\ 0.3305 + 1.4671i & 0.4826 - 2.7875i & 0.2590 + 1.0407i \\ 0.2414 + 1.1917i & 0.2590 + 1.0407i & 0.3104 - 2.4030i \end{bmatrix} \quad (5.22)$$

$$Y_{loaddecrease} = \begin{bmatrix} 0.8150 - 2.9619i & 0.2409 + 1.5520i & 0.1758 + 1.2545i \\ 0.2409 + 1.5520i & 0.3524 - 2.6684i & 0.1638 + 1.1290i \\ 0.1758 + 1.2545i & 0.1638 + 1.1290i & 0.2408 - 2.3376i \end{bmatrix} \quad (5.23)$$

Simulation Results

From the response of angle deviations $(\delta_2 - \delta_1)$ and $(\delta_3 - \delta_1)$ in figures 5.29 and 5.30, it is shown that with an increase and decrease of 50% in the load on bus-8, the system is settled to the steady state at 1.55 s and 1.62 s respectively. The angle deviations $(\delta_2 - \delta_1)$ and $(\delta_3 - \delta_1)$ are brought to the the new steady state values 0.32 rad and 0.91 rad when the load increased by 50% and to the values 0.27 rad and 0.18 rad when the load decreased by 50%.

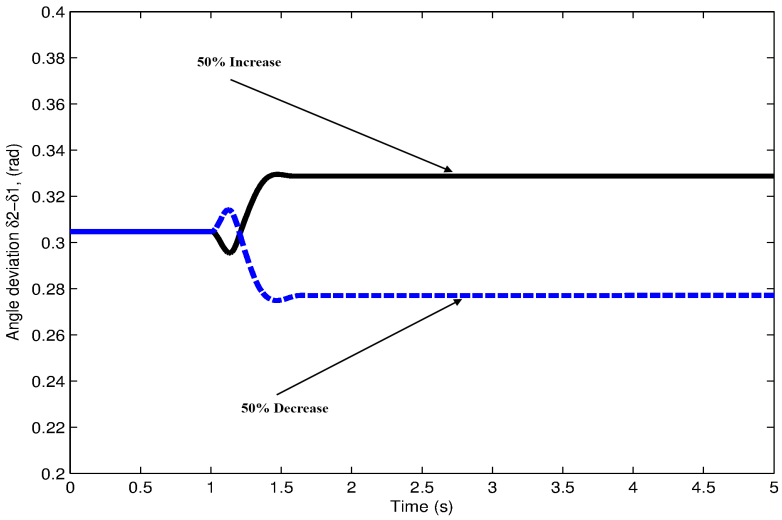

Figure 5.29: Angle deviation $(\delta_2 - \delta_1)$ of load change bus-8.

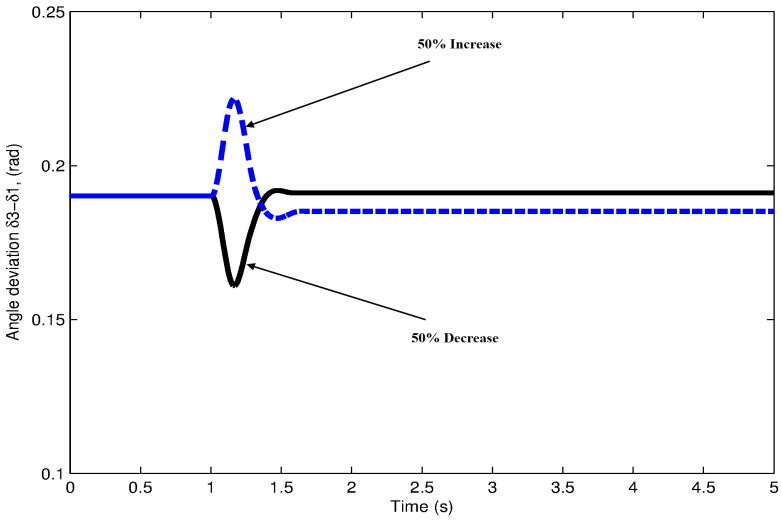

Figure 5.30: Angle deviation $(\delta_3 - \delta_1)$ of load change bus-8.

In figures 5.31 and 5.32 , the speed deviations $(\omega_2 - \omega_1)$ and $(\omega_3 - \omega_1)$ of MMPS are brought to zero at 1.6 s when the load increased by 50% and 1.7 s when the load decreased by 50%.

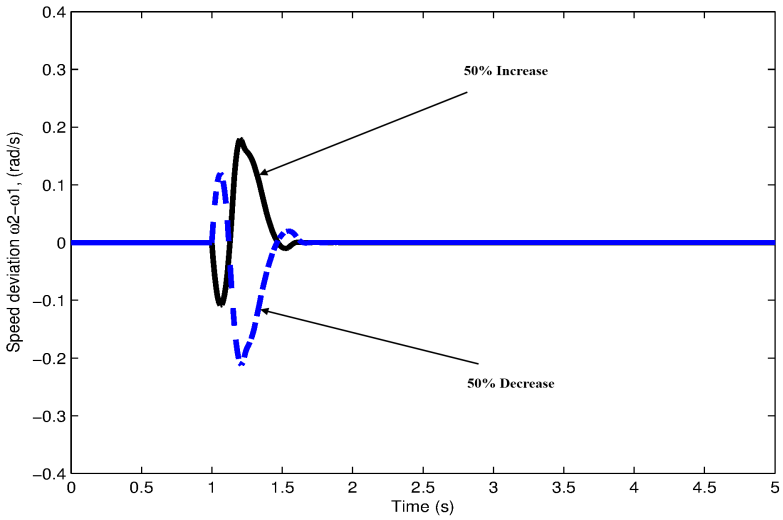

Figure 5.31: Speed deviation $(\omega_2 - \omega_1)$ of load change bus-8.

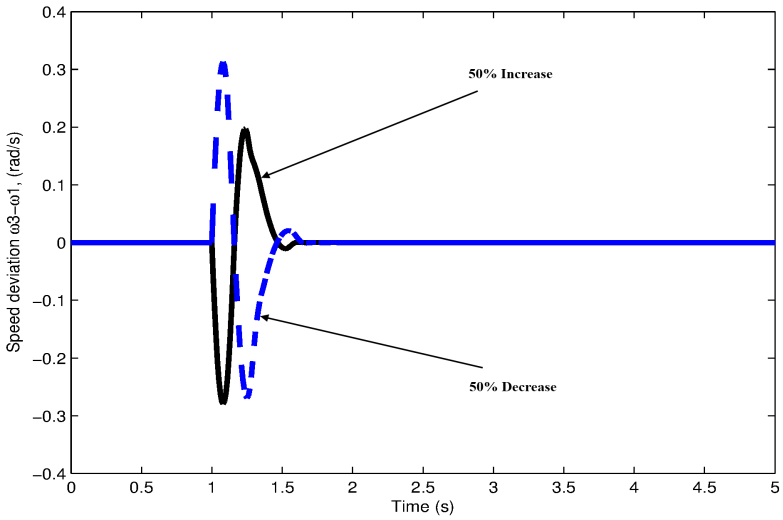

Figure 5.32: Speed deviation $(\omega_3 - \omega_1)$ of load change bus-8.

For comparison between the three cases of load changing, the speed deviation of three cases are illustrated in figures 5.33, 5.34, 5.35, and 5.36.

When the load change takes place in bus-8 the dynamical performance of MMPS has the best settling time (1.6 s in the case of increasing the load and 1.7 s in the

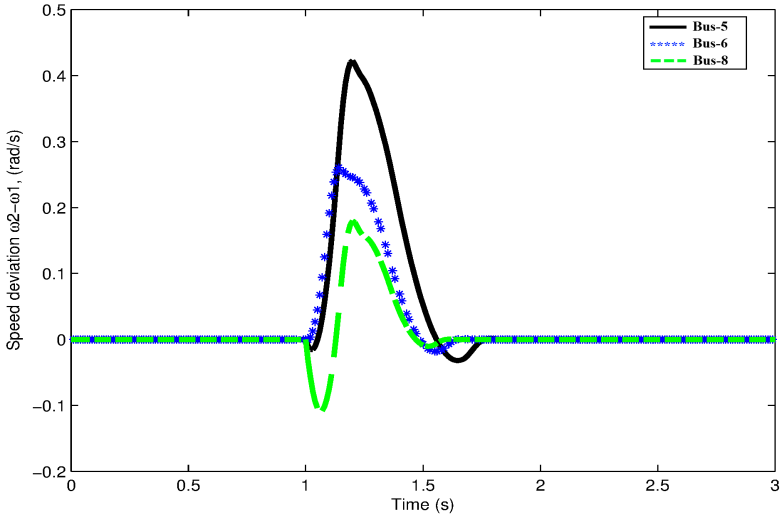

Figure 5.33: Speed deviation ($\omega_2 - \omega_1$) of 50% increase on buses (bus-5,bus-6, and bus-8).

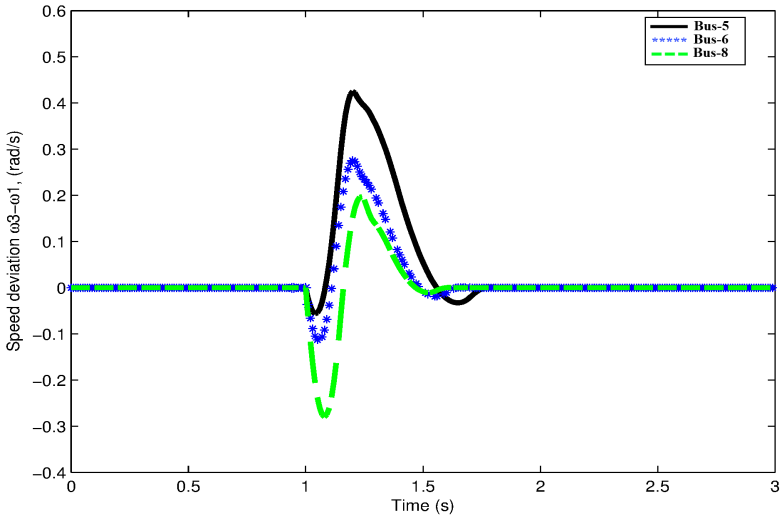

Figure 5.34: Speed deviation ($\omega_3 - \omega_1$) of 50% increase on buses (bus-5,bus-6, and bus-8).

case of decreasing the load) and it has the lowest overshoot. On the other hand, when the load change takes place in bus-5, the dynamical performance of MMPS has the longest settling time (1.82 s in the case of increasing the load and 2.05 s in the case of decreasing the load) and it has the highest overshoot.

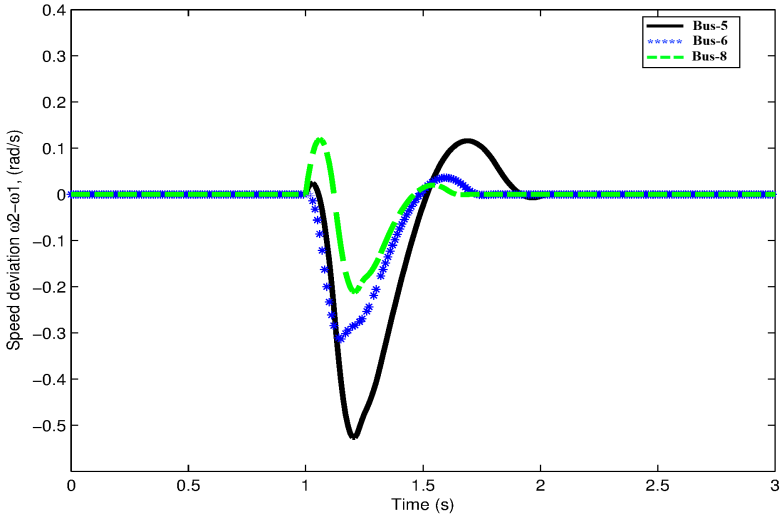

Figure 5.35: Speed deviation ($\omega_2 - \omega_1$) of 50% decrease on buses (bus-5,bus-6, and bus-8).

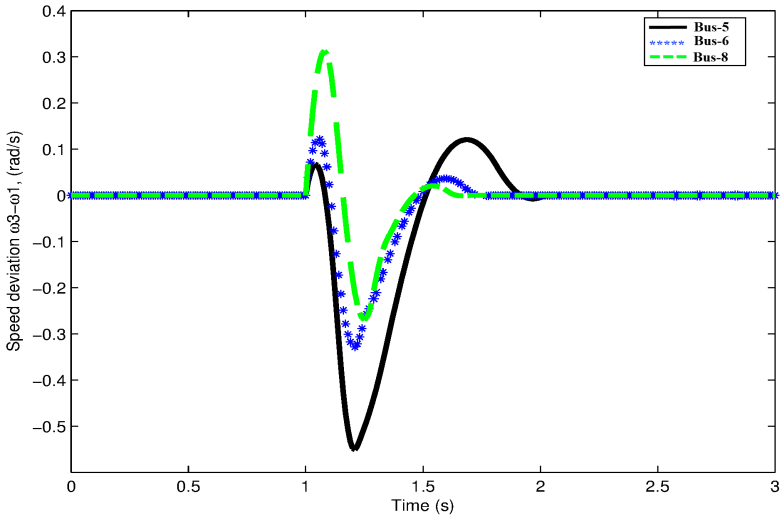

Figure 5.36: Speed deviation ($\omega_3 - \omega_1$) of 50% decrease on buses (bus-5,bus-6, and bus-8).

5.4 Mechanical Power Changing

Mechanical power (P_m) of each machine is considered constant for all previous cases as stated in prior assumptions. In this case, a 5% step change is applied in

mechanical power for each machine of the 3-Machines 9-bus WSCC system. This step change of mechanical power may come from the sudden change in steam valve (steam turbine) or gate (hydraulic turbine).

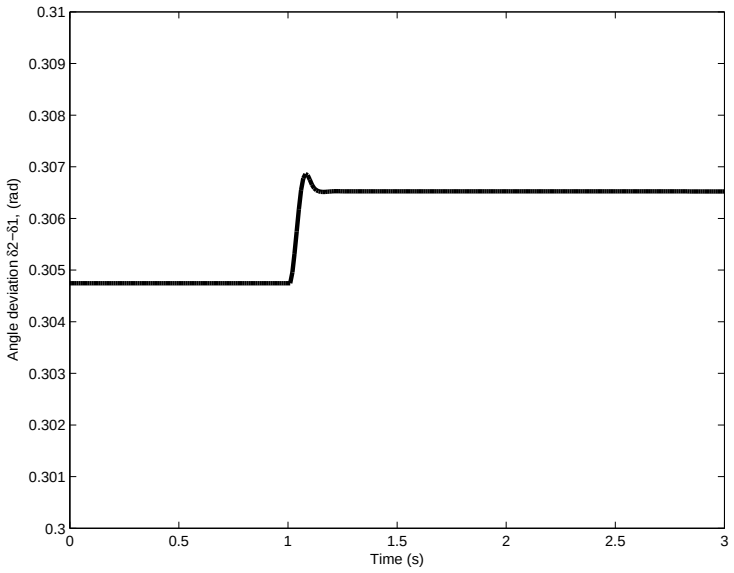

Figure 5.37: Angle deviation ($\delta_2 - \delta_1$) of Mechanical Power change.

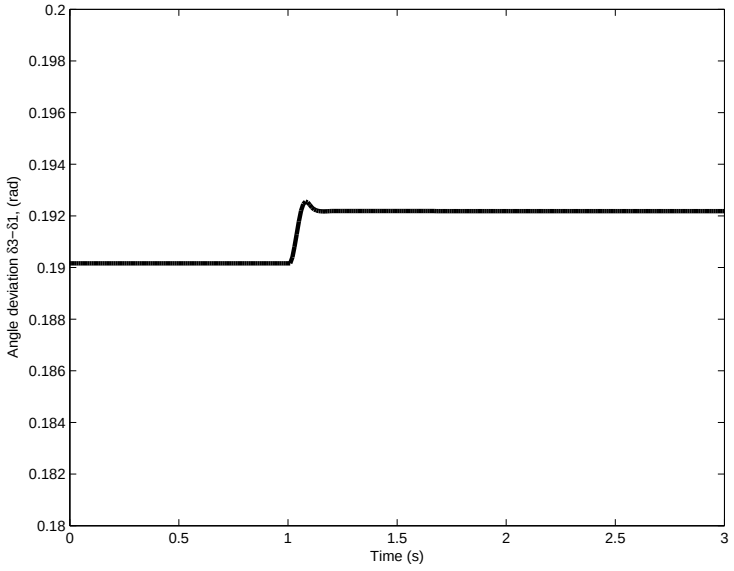

Figure 5.38: Angle deviation ($\delta_3 - \delta_1$) of Mechanical Power change.

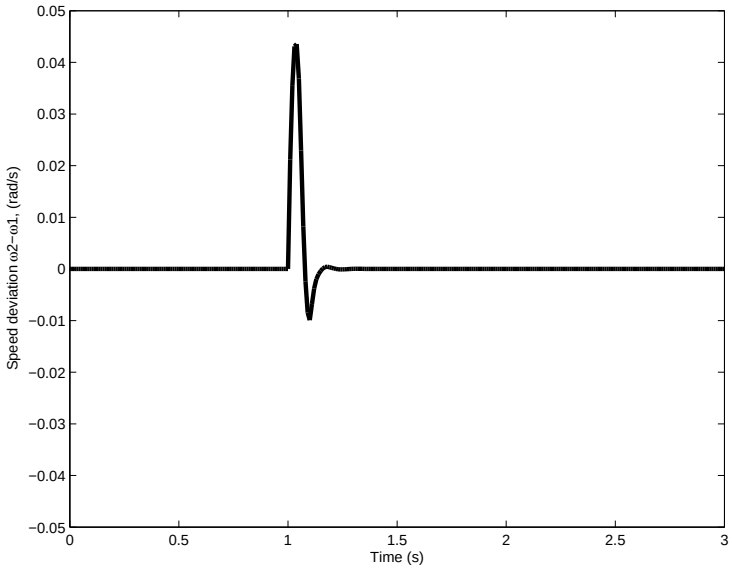

Figure 5.39: Speed deviation $(\omega_2 - \omega_1)$ of Mechanical Power change.

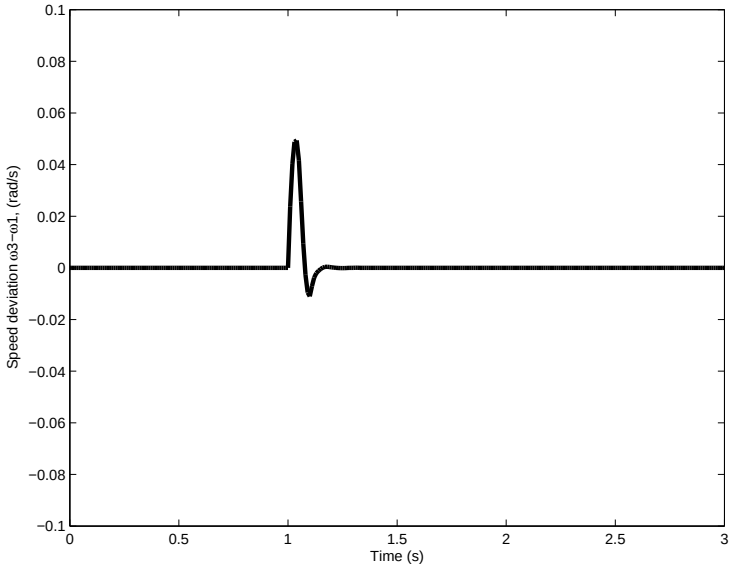

Figure 5.40: Speed deviation $(\omega_3 - \omega_1)$ of Mechanical Power change.

Simulation Results

From figures 5.37 and 5.38 it is seen that the angle deviations $(\delta_2 - \delta_1)$ and $(\delta_3 - \delta_1)$ reached the steady state with values 0.3065 rad and 0.1922 rad respectively. These values are differ slightly from the previous steady state. The settling time

of both angle deviations is 1.15 s.

The speed deviations $(\omega_2 - \omega_1)$ and $(\omega_3 - \omega_1)$ in figures 5.39 and 5.40 settled to zero at 1.21 s. The speed deviation $(\omega_2 - \omega_1)$ reached a maximum value of 0.043 rad/s at 1.04 s, whereas, the speed deviation $(\omega_3 - \omega_1)$ reached a maximum value of 0.049 rad/s at 1.04 s.

It can be seen that, although the system has a disturbance in mechanical power for each machine, the NMPC controller is still capable of stabilizing the system and bringing it back to the operating frequency (60 Hz).

CHAPTER 6

CONCLUSIONS AND FUTURE WORK

6.1 Conclusions

The main points that can be concluded from this thesis are:

1. The Active set algorithm is used with Model Predictive Control to control the power systems like SMIB and MMPS which have inequality physical constraints.

2. The NMPC controller is applied to the nonlinear model of the power systems with no need for any linearization or transformation techniques and with no help of FACTS devices or any other supported controllers.

3. NMPC control emphasized that the constraints are satisfied for both Single Machine Infinite Bus and Multi-machine Power System.

4. The results of the application of the NMPC controller showed that the NMPC controller is successfully able to enhance the dynamical performance of SMIB and MMPS systems. The results of this work are better than what was achieved in previous work on the same topic.

5. Under the three phase fault, the transient stability of the Multi-machine Power System is enhanced using NMPC controller. Despite the change of fault place, the NMPC controller is still able to bring the MMPS to steady state.

6. The dynamical performance of MMPS is examined by substantial changes in the load. The response showed that the NMPC controller stabilized the system and it depends on the place of load buses as well.

7. NMPC controller is able to bring the MMPS system to steady state when a sudden change took place in the mechanical power of each machine.

8. The robustness of the proposed controller has been examined against the variations of system parameters.

6.2 Future Work

The research in this subject can be further developed in a number of ways:

1. The dynamics of the governor can be considered in this work which means the mechanical power is no longer constant as stated in the MMPS assumptions.

2. The proposed cost function can be formulated in different ways in order to investigate the performance of the NMPC controller.

3. Different types of optimization methods rather than active set can be used.

4. The effects of MPC tuning parameters on the dynamical performance of MMPS can be investigated.

5. Study the performance of MMPS under other large disturbances like switching of lines or loss of one generator.

6. The real-time optimization complexity can be improved by using high speed processors or by using other fast techniques of optimization.

7. This work can be further applied to large networks of power systems.

REFERENCES

[1] G. Matthews, R. DeCarlo, P. Hawley, and S. Lefebvre, "Toward a feasible variable structure control design for a synchronous machine connected to an infinite bus," *IEEE Transactions on Automatic Control*, vol. 31, no. 12, pp. 1159–1163, 1986.

[2] N. Yadaiah and N. Venkata Ramana, "Linearisation of multi-machine power system: Modeling and control - a survey," *International Journal of Electrical Power and Energy Systems*, vol. 29, no. 4, pp. 297–311, 2007.

[3] F. DeMello and C. Concordia, "Concepts of synchronous machine stability as affected by excitation control," *IEEE Transactions on Power Apparatus and Systems*, vol. PAS-88, no. 4, pp. 316–329, 1969.

[4] Y.-N. Yu and H. A. M. Moussa, "Optimal stabilization of a multi-machine system," *IEEE Transactions on Power Apparatus and Systems*, vol. PAS-91, no. 3, pp. 1174–1182, 1972.

[5] J. Ritonja, D. Dolinar, and B. Grcar, "Simple adaptive control for a power-system stabiliser," *Control Theory and Applications, IEE Proceedings* -,

vol. 147, no. 4, pp. 373–380, 2000.

[6] Y. Cao, L. Jiang, S. Cheng, D. Chen, O. P. Malik, and G. Hope, "A nonlinear variable structure stabilizer for power system stability," *IEEE Transactions on Energy Conversion*, vol. 9, no. 3, pp. 489–495, 1994.

[7] S. Bhil, A. Kamath, N. Singh, and S. Wagh, "Transient stability enhancement of power system using mpc based tcsc controller," in *Power and Energy Society General Meeting*, pp. 1–7, 2009.

[8] T. Nguyen and S. Wagh, "Model predictive control of facts devices for power system transient stability," in *Transmission Distribution Conference Exposition: Asia and Pacific*, pp. 1–4, 2009.

[9] T. Nguyen and S. Wagh, "Predictive control-based facts devices for power system transient stability improvement," in *Advances in Power System Control, Operation and Management (APSCOM 2009), on 8th International Conference*, pp. 1–6, 2009.

[10] C. Venkatesh, T. Deepak, K. Rajesh, K. Krishna, and A. K. Kamath, "Flatness based tcsc controller for transient stability enhancement of power system," in *Proceedings - International Symposium: Modern Electric Power Systems*, 2010.

[11] B. Ahmadzade, G. Shahgholian, F. M. Tehrani, and M. Mahdavian, "Model predictive control to improve power system oscillations of smib with fuzzy

logic controller," in *International Conference on Electrical Machines and Systems*, 2011.

[12] B. P. Gibbs, D. S. Weber, and D. W. Porter, "Application of nonlinear model-based predictive control to fossil power plants," in *Proceedings of the IEEE Conference on Decision and Control*, vol. 2, pp. 1850–1856, 1991.

[13] B. P. Gibbs, "Nonlinear model predictive control for fossil power plants," in *Proceedings of the American Control Conference*, vol. 4, pp. 3091–3098, 1992.

[14] J. . Xiao and X. . Wang, "Nonlinear neural network predictive control for power unit using particle swarm optimization," in *Proceedings of the 2006 International Conference on Machine Learning and Cybernetics*, pp. 2851–2856, 2006.

[15] A. Koerber and R. King, "Nonlinear model predictive control for wind turbines," in *European Wind Energy Conference and Exhibition*, pp. 285–287, 2011.

[16] D. Q. Dang, Y. Wang, and W. Cai, "Nonlinear model predictive control (nmpc) of fixed pitch variable speed wind turbine," in *2008 IEEE International Conference on Sustainable Energy Technologies*, pp. 29–33, 2008.

[17] D. Q. Dang, Y. Wang, and W. Cai, "A multi-objective optimal nonlinear control of variable speed wind turbine," in *2009 IEEE International Conference on Control and Automation*, pp. 17–22, 2009.

[18] L. C. Henriksen, N. K. Poulsen, and M. H. Hansen, "Nonlinear model predictive control of a simplified wind turbine," in *IFAC Proceedings Volumes*, vol. 18, pp. 551–556, 2011.

[19] R. Horalek and L. Imsland, "Nonlinear model predictive control of a benchmark nonlinear boiler," in *2011 23rd International Symposium on Information, Communication and Automation Technologies*, pp. 1–6, 2011.

[20] S. G. Abokhatwa and M. R. Katebi, "Nonlinear predictive control of an industrial power plant boiler," in *2012 20th Mediterranean Conference on Control and Automation*, pp. 1223–1228, 2012.

[21] F. Tahami, M. R. Abedi, and K. Rezaei, "Optimum nonlinear model predictive controller design for flyback pfc rectifiers," in *2010 IEEE Symposium on Industrial Electronics and Applications*, pp. 70–75, 2010.

[22] M. Abedi, B. . Song, and B. Ernzen, "Optimum tracking of nonlinear-model predictive control for boost based pfc rectifier," in *Proceedings of the Annual Southeastern Symposium on System Theory*, pp. 87–91, 2011.

[23] M. Lazar, W. P. M. H. Heemels, B. J. P. Roset, H. Nijmeijer, and P. P. J. Van Den Bosch, "Input-to-state stabilizing sub-optimal nmpc with an application to dc-dc converters," *International Journal of Robust and Nonlinear Control*, vol. 18, no. 8, pp. 890–904, 2008.

[24] M. Yousuf, "Nonlinear Predictive Control Using Particle Swarm Optimization: Application to Power Systems," Master's thesis, King Fahd University of Petroleum and Minerals Dhahran, Jun 2009.

[25] M. S. Yousuf, S. Z. Rizvi, and H. N. Al-Duwaish, "Intelligent predictive control methods for synchronous power system," in *2011 IEEE Symposium on Computational Intelligence in Control and Automation*, pp. 67–73, 2011.

[26] S. R. Wagh, A. K. Kamath, and N. M. Singh, "Non-linear model predictive control for improving transient stability of power system using tcsc controller," in *Proceedings of 2009 7th Asian Control Conference*, pp. 1627–1632, 2009.

[27] S. R. Wagh, A. K. Kamath, and N. M. Singh, "A nonlinear tcsc controller based on control lyapunov function and receding horizon strategy for power system transient stability improvement," in *2009 IEEE International Conference on Control and Automation*, pp. 813–818, 2009.

[28] H. I. Shaheen, G. I. Rashed, and S. J. Cheng, "Nonlinear optimal predictive controller for static synchronous compensator (statcom)," in *Transmission and Distribution Exposition Conference: 2008 IEEE PES Powering Toward the Future*, 2008.

[29] E. Larsen and D. A. Swann, "Applying power system stabilizers part i: General concepts," *IEEE Transactions on Power Apparatus and Systems*, vol. PAS-100, no. 6, pp. 3017–3024, 1981.

[30] J. Kanniah, O. P. Malik, and G. S. Hope, "Excitation control of synchronous generators using adaptive regulators. part i - theory and simulation results.," *IEEE transactions on power apparatus and systems*, vol. PAS-103, no. 5, pp. 897–903, 1984.

[31] J. H. Chow and J. J. Sanchez-Gasca, "Pole-placement designs of power system stabilizers," *IEEE Transactions on Power Systems*, vol. 4, no. 1, pp. 271–277, 1989.

[32] D. Ostojic and B. Kovacevic, "On the eigenvalue control of electromechanical oscillations by adaptive power system stabilizer," *IEEE Transactions on Power Systems*, vol. 5, no. 4, pp. 1118–1126, 1990.

[33] R. J. Fleming and J. Sun, "Optimal multivariable stabilizer for a multimachine plant," *IEEE Transactions on Energy Conversion*, vol. 5, no. 1, pp. 15–22, 1990.

[34] J. Talaq, "Optimal power system stabilizers for multi machine systems," *International Journal of Electrical Power and Energy Systems*, vol. 43, no. 1, pp. 793–803, 2012.

[35] G. P. Chen, O. P. Malik, G. S. Hope, Y. H. Qin, and G. Y. Xu, "Adaptive power system stabilizer based on the self-optimizing pole shifting control strategy," *IEEE Transactions on Energy Conversion*, vol. 8, no. 4, pp. 639–645, 1993.

[36] Y. M. Park and W. Kim, "Discrete-time adaptive sliding mode power system stabilizer with only input/output measurements," *International Journal of Electrical Power and Energy Systems*, vol. 18, no. 8, pp. 509–517, 1996.

[37] M. Hunjan and G. Venayagamoorthy, "Adaptive power system stabilizers using artificial immune system," in *IEEE Symposium on Artificial Life*, pp. 440–447, 2007.

[38] H. Ukai, M. Makino, S. Cui, H. Kandoh, and H. Fujita, "Decentralized H_∞ control for stabilizing multi-machine power systems," in *Fourth International Conference on Advances in Power System Control, Operation and Management*, vol. 2, pp. 421–426, 1997.

[39] M. Dehghani and S. K. Nikravesh, "Lyapunov based H_∞ controller design in multimachine power systems," in *11th International Conference on Control, Automation, Robotics and Vision*, pp. 1667–1672, 2010.

[40] V. G. D. C. Samarasinghe and N. Pahalawaththa, "Damping of multimodal oscillations in power systems using variable structure control techniques," *Generation, Transmission and Distribution, IEE Proceedings-*, vol. 144, no. 3, pp. 323–331, 1997.

[41] J. Fernández-Vargas and G. Ledwich, "Variable structure control for power systems stabilization," *International Journal of Electrical Power and Energy Systems*, vol. 32, no. 2, pp. 101–107, 2010.

[42] M. A. Abido, "Particle swarm optimization for multimachine power system stabilizer design," in *Proceedings of the IEEE Power Engineering Society Transmission and Distribution Conference*, vol. 3, pp. 1346–1351, 2001.

[43] K. El-Metwally and O. P. Malik, "Application of fuzzy logic stabilisers in a multimachine power system environment," *Generation, Transmission and Distribution, IEE Proceedings-*, vol. 143, no. 3, pp. 263–268, 1996.

[44] H. Alkhatib and J. Duveau, "Dynamic genetic algorithms for robust design of multimachine power system stabilizers," *International Journal of Electrical Power and Energy Systems*, vol. 45, no. 1, pp. 242–251, 2013.

[45] L. Yi-qun, Tenglin, L. Wang-shun, and L. Jian-fei, "The study on real-time transient stability emergency control in power system," in *Canadian Conference on Electrical and Computer Engineering*, vol. 1, pp. 138–143, 2002.

[46] A. Soos and O. P. Malik, "Robust multi-model based control," in *Power India Conference*, 2006.

[47] B. Wu and O. P. Malik, "Multivariable adaptive control of synchronous machines in a multimachine power system," *IEEE Transactions on Power Systems*, vol. 21, no. 4, pp. 1772–1781, 2006.

[48] H. Ye and Y. Liu, "Wide-area model predictive damping controller based on online recursive closed-loop subspace identification," in *International Conference on Power System Technology: Technological Innovations Making Power Grid Smarte*, 2010.

[49] D. Wang, M. Glavic, and L. Wehenkel, "A new mpc scheme for damping wide-area electromechanical oscillations in power systems," in *PowerTech*, 2011.

[50] X. Du, D. Ernst, and P. Crossley, "A model predictive based emergency control scheme using tcsc to improve power system transient stability," in *Power and Energy Society General Meeting*, pp. 1–7, 2012.

[51] D. Wang, M. Glavic, and L. Wehenkel, "Distributed mpc of wide-area electromechanical oscillations of large-scale power systems," in *International Conference on Intelligent System Application to Power Systems (ISAP)*, pp. 1–7, 2011.

[52] M. Moradzadeh, L. Bhojwani, and R. Boel, "Coordinated voltage control via distributed model predictive control," in *Chinese Control and Decision Conference (CCDC)*, pp. 1612–1618, 2011.

[53] M. Moradzadeh, R. Boel, and L. Vandevelde, "Voltage coordination in multi-area power systems via distributed model predictive control," *IEEE Transactions on Power Systems*, vol. 28, no. 1, pp. 513–521, 2013.

[54] Y. Qudaih, Y. Mitani, and T. Mohamed, "Wide-area power system oscillation damping using robust control technique," in *Asia-Pacific Power and Energy Engineering Conference (APPEEC)*, pp. 1–4, 2012.

[55] E. Bijami, J. Askari, and M. Farsangi, "Design of stabilising signals for power system damping using generalised predictive control optimised by a new hy-

brid shuffled frog leaping algorithm," *Generation, Transmission Distribution*, vol. 6, no. 10, pp. 1036–1045, 2012.

[56] V. Rajkumar and R. R. Mohler, "Nonlinear predictive control for the damping of multimachine power system transients using facts devices," in *Proceedings of the IEEE Conference on Decision and Control*, vol. 4, pp. 4074–4079, 1994.

[57] M. Zima and G. Andersson, "Model predictive control employing trajectory sensitivities for power systems applications," in *Proceedings of the 44th IEEE Conference on Decision and Control, and the European Control Conference*, pp. 4452–4456, 2005.

[58] M. Larsson, D. J. Hill, and G. Olsson, "Emergency voltage control using search and predictive control," *International Journal of Electrical Power and Energy Systems*, vol. 24, no. 2, pp. 121–130, 2002.

[59] J. J. Ford, G. Ledwich, and Z. Y. Dong, "Efficient and robust model predictive control for first swing transient stability of power systems using flexible ac transmission systems devices," *IET Generation, Transmission and Distribution*, vol. 2, no. 5, pp. 731–742, 2008.

[60] J. Richalet, A. Rault, J. Testud, and J. Papon, "Model predictive heuristic control: Applications to industrial processes," *Automatica*, vol. 14, no. 5, pp. 413 – 428, 1978.

[61] C. Cutler and B. Ramaker, "Dynamic matrix control–a computer control algorithm," in *Proc. Joint Automatic Control Conference*, 1980.

[62] D. Clarke, C. Mohtadi, and P. Tuffs, "Generalized predictive control-part i. the basic algorithm," *Automatica*, vol. 23, no. 2, pp. 137–148, 1987.

[63] C. Garcia and M. Morarl, "Internal model control. 1. a unifying review and some new results," *Industrial and Engineering Chemistry Process Design and Development*, vol. 21, no. 2, pp. 308–323, 1982.

[64] R. Soeterboek, *Predictive Control - A Unified Approach.* Prentice Hall, 1992.

[65] R. D. Keyser, P. V. de Velde, and F. Dumortier, "A comparative study of self-adaptive long-range predictive control methods," *Automatica*, vol. 24, no. 2, pp. 149 – 163, 1988.

[66] C. E. García, D. M. Prett, and M. Morari, "Model predictive control: Theory and practice—a survey," *Automatica*, vol. 25, no. 3, pp. 335 – 348, 1989.

[67] M. Morari and J. H. Lee, "Model predictive control: past, present and future," *Computers and Chemical Engineering*, vol. 23, no. 4–5, pp. 667 – 682, 1999.

[68] L. Wang, *Model Predictive Control System Design and Implementation Using Matlab®*. Springer Verlag, 2009.

[69] E. F. Camacho, C. Bordons, E. F. Camacho, and C. Bordons, *Model predictive control*, vol. 2. Springer London, 2004.

[70] S. J. Qin and T. A. Badgwell, "An overview of industrial model predictive control technology," in *AIChE Symposium Series*, vol. 93, pp. 232–256, 1997.

[71] S. J. Qin and T. A. Badgwell, "An overview of nonlinear model predictive control applications," in *Nonlinear Model Predictive Control*, pp. 369–392, Springer, 2000.

[72] C. C. Chen and L. Shaw, "On receding horizon feedback control.," pp. 377–382, 1982.

[73] A. A. Patwardhan, G. T. Wright, and T. F. Edgar, "Nonlinear model-predictive control of distributed-parameter systems," *Chemical Engineering Science*, vol. 47, no. 4, pp. 721 – 735, 1992.

[74] R. Kawathekar and J. B. Riggs, "Nonlinear model predictive control of a reactive distillation column," *Control Engineering Practice*, vol. 15, no. 2, pp. 231 – 239, 2007.

[75] J. Albuquerque, V. Gopal, G. Staus, L. T. Biegler, and B. Ydstie, "Interior point SQP strategies for large-scale, structured process optimization problems," *Computers and Chemical Engineering*, vol. 23, no. 4–5, pp. 543 – 554, 1999.

[76] C. Onnen, R. Babuška, U. Kaymak, J. Sousa, H. Verbruggen, and R. Isermann, "Genetic algorithms for optimization in predictive control," *Control Engineering Practice*, vol. 5, no. 10, pp. 1363 – 1372, 1997.

[77] H. Al-Duwaish and W. Naeem, "Nonlinear model predictive control of hammerstein and wiener models using genetic algorithms," in *Proceedings of the IEEE International Conference on Control Applications*, pp. 465–469, 2001.

[78] A. Zheng, "A computationally efficient nonlinear mpc algorithm," in *Proceedings of the American Control Conference*, vol. 3, pp. 1623–1627 vol.3, 1997.

[79] M. A. Henson, "Nonlinear model predictive control: Current status and future directions," *Computers and Chemical Engineering*, vol. 23, no. 2, pp. 187–202, 1998.

[80] D. Q. Mayne, J. B. Rawlings, C. V. Rao, and P. O. M. Scokaert, "Constrained model predictive control: Stability and optimality," *Automatica*, vol. 36, no. 6, 2000.

[81] J. B. Rawlings, "Tutorial overview of model predictive control," *IEEE Control Systems Magazine*, vol. 20, no. 3, pp. 38–52, 2000.

[82] F. Allgöwer, R. Findeisen, and Z. K. Nagy, "Nonlinear model predictive control: From theory to application," *Journal of the Chinese Institute of Chemical Engineers*, vol. 35, no. 3, pp. 299–315, 2004.

[83] L. Grüne and J. Pannek, *Nonlinear Model Predictive Control Theory and Algorithms*. Springer, 2011.

[84] R. Findeisen and F. Allgöwer, "An introduction to nonlinear model predictive," in *21st Benelux Meeting on Systems and Control, Veidhoven*, pp. 1–23, 2002.

[85] J. Nocedal and S. J. Wright, "Numerical optimization, second edition," *Numerical optimization*, pp. 497–528, 2006.

[86] R. A. Bartlett, A. Wachter, and L. Biegler, "Active set vs. interior point strategies for model predictive control," in *Proceedings of the American Control Conference*, vol. 6, pp. 4229–4233, 2000.

[87] M. Cannon, B. Kouvaritakis, and J. Rossiter, "Efficient active set optimization in triple mode mpc," in *Proceedings of the American Control Conference*, vol. 3, pp. 2382–2387, 2001.

[88] L. Wirsching, H. Ferreau, H. Bock, and M. Diehl, "An online active set strategy for fast adjoint based nonlinear model predictive control," vol. 7, pp. 234–239, 2007.

[89] B. Muller and P. De Vaal, "Development of a model predictive controller for a milling circuit," *Journal-South African Institute of Mining and Metallurgy*, vol. 100, no. 7, pp. 449–454, 2000.

[90] A. Chianese and H. J. Kramer, *Industrial crystallization process monitoring and control*. John Wiley & Sons, 2012.

[91] A. Hugo, "Limitations of model predictive controllers," *Hydrocarbon Preocessing*, vol. 79, no. 1, 2000.

[92] M. Diehl, H. Bock, J. P. Schlöder, R. Findeisen, Z. Nagy, and F. Allgöwer, "Real-time optimization and nonlinear model predictive control of processes governed by differential-algebraic equations," *Journal of Process Control*, vol. 12, no. 4, pp. 577 – 585, 2002.

[93] P. Anderson and A. Fouad, *Power system control and stability.* New Jersey: IEEE press, 1994.

[94] K. Padiyar, *Power system dynamics stability and control.* BS publications, 2008.

[95] P. Sauer and M. Pai, *Power system dynamics and stability.* India: Pearson Education, 2002.

[96] H. Saadat, *Power system analysis.* WCB/McGraw-Hill Singapore, 1999.

Vitae

- Name: Mohammed Mansoor Bin Thabit
- Nationality: Yemeni
- Date of Birth: 16/02/1981
- Academic Background: Received Bachelor's degree in Electrical and Electronics Engineering from the Hadhramout University of Science and Technology, Mukalla, Yemen in June 2007. Completed Master's degree requirements at King Fahd University of Petroleum and Minerals in December 2013.
- Work Experience:
    1. Field Operator with Weatherford Company-Total Project-Block10-Yemen (16/08/2009-24/06/2010).
    2. Early Well Test (EWT) Operator with Weatherford Company-Total Project-Block10-Yemen (25/12/2007-16/08/2009).
    3. Teacher in Secondary School-Qa'uda,Yemen (10/9/2007-23/12/2007).
- Publications: Omar AI-Buraiki and Mohammed Bin Thabit, "Model Predictive Control Design Approach for Autonomous Bicycle Kinematics Stabilization," *in the 22nd Mediterranean Conference on Control and Automation*, 2014.

- Email: *moh.binthabit@gmail.com.*
- Mobile: +966559450318.
- Permanent Address: KFUPM main campus building 819 room 230.